Perovskite-Organic Tandem Solar Cells

Brinkmann, K.O.[1,2,†] *; Wang, P.[1,2,†] *; Lang, F.[3]; Li, W[4]; Guo, X.[5,6]; Zimmermann, F.[1,2]; Olthof, S.[7]; Neher, D.[3]; Hou, Y.[5,6]; Stolterfoht, M.[8]; Wang, T.[4] *; Djurišić, A. B.[9]; Riedl, T.[1,2] *

Affiliations:

1. Institute of Electronic Devices, University of Wuppertal, Wuppertal, Germany
2. Wuppertal Center for Smart Materials & Systems, University of Wuppertal, Wuppertal, Germany
3. Soft Matter Physics and Optoelectronics, University of Potsdam, Potsdam, Germany
4. School of Materials Science and Engineering, Wuhan University of Technology, Wuhan, China
5. Solar Energy Research Institute of Singapore, National University of Singapore, Singapore
6. Department of Chemical and Biomolecular Engineering, National University of Singapore, Singapore
7. Department of Chemistry, University of Cologne, Cologne, Germany
8. Electronic Engineering Department, The Chinese University of Hong Kong, Hong Kong
9. Department of Physics, University of Hong Kong, Hong Kong

* corresponding

† equal contribution

Abstract:

Halide perovskites overwhelmed the field of photovoltaics with unprecedented progress in efficiency. Their facile bandgap tunability renders perovskite solar cells excellent building-blocks for multi-junction architectures, that provide the prospect to overcome fundamental efficiency limits of single-junctions. Simultaneously, the area of organic solar cells has seen tremendous advances by the introduction of non-fullerene acceptors. Organic and perovskite semiconductors share similar processing technologies, which makes them attractive partners in multi-junction architectures. This Perspective article sheds light on the prospects and challenges of perovskite-organic tandem solar cells by highlighting the key aspects of the individual building blocks and their interplay in the tandem. Specifically, the role of non-fullerene acceptors in efficient narrow-gap organic solar cells with high operational stability is discussed. A further focus is the wide-gap perovskite solar cell, where long term stability is the most pressing issue that needs attention. Eventually, the design and functionality of high-quality interconnects are outlined along with a view on its impacts on the characteristics of the tandem. In the end, the prospects of perovskite-organic tandem solar cells are benchmarked against other emerging tandem solar cell technologies.

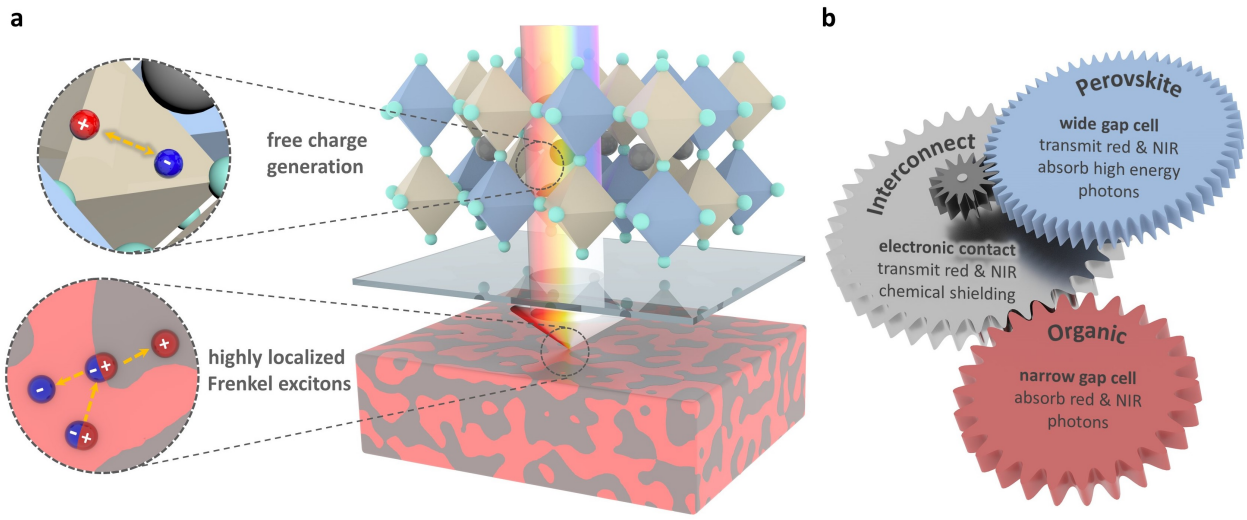

Figure 1: General working principle of perovskite-organic tandem solar cells. a, *Charge generation in perovskite and organic solar cells. While in most three-dimensional perovskite absorbers, that are typically used for solar cells (top), free charge carriers are created upon light absorption, the primary excitations in organic semiconductors are tightly bound Frenkel excitons that must be split at a donor-acceptor interface* ***b,*** *Role of the subcells and the interconnect.*

Introduction

Since their introduction, metal-halide perovskite solar cells have achieved stunning efficiency levels, that are now at par with that of established photovoltaic technologies.[1] Upon further progress, however, perovskite solar cells will be approaching fundamental efficiency limits that generally apply for single junction cells.[2] Consequently, there is an increasing interest in tandem architectures, that allow to surpass the so-called detailed-balance limit of single junctions by combining two solar cells with different absorption onsets. Thereby, thermalization losses can be reduced, which results in a more efficient conversion of the incident solar power into electricity.[3] As shown in Figure 1, monolithic tandem devices typically consist of three building blocks: a solar cell with a wide energy gap that absorbs high-energy photons, a solar cell with a narrow energy gap that absorbs the transmitted low-energy photons, and an optically transparent interconnect that establishes an electrical contact between both subcells. Like in III/V semiconductors, the bandgap of perovskite semiconductors can be widely varied through their composition. For tandem devices their absorption properties can therefore be easily adapted to a range of narrow-gap solar cells, such as silicon, copper-indium-gallium selenide (CIGS), and narrow-bandgap perovskite subcells. The recent success of highly efficient organic solar cells with absorption spectra reaching well into the infrared, extended the portfolio of efficient partners to form a tandem with perovskite wide-gap cells. This development led to very exciting advances in perovskite-organic tandem solar cells over the past three years, with efficiencies increasing from below 17% to above 24%.[4-6] The focus of this perspective is on the specific challenges and opportunities that arise from combining these two emerging thin film photovoltaic technologies, i.e. perovskite and organic solar cells, into a monolithic tandem device. As depicted in Figure 1a, both technologies rely on fundamentally different mechanisms for the generation of free charge carriers upon illumination, related in part to their vastly different electric permittivity. Owing to the typically low exciton binding energy of many high permittivity perovskite absorbers, free charge carriers are generated directly upon light absorption at room temperature. In organic absorbers with low permittivity, strongly localized Frenkel excitons with higher binding energy are formed, that need to be dissociated at a hetero interface of two different organic moieties. This perspective will address the most relevant aspects of each building block with respect to their application

in tandem cells with the goal to benchmark the perovskite-organic tandem technology against other emerging tandem concepts and to identify the most important levers for further progress.

Box 1: The emergence of Y-type non-fullerene acceptors:

For a considerable time, the development of organic solar cells was linked to the use of fullerene derivatives as electron acceptors (A) in blends, usually in combination with a polymer-based electron donor (D), to form so-called bulk-heterojunction networks.[7] Such a structure is needed to afford efficient exciton dissociation at the internally distributed donor-acceptor interfaces competing against exciton decay to the ground state. Around 2012, after more than a decade of continuous optimization, the progress in power conversion efficiency levelled off at a value slightly above 10%.

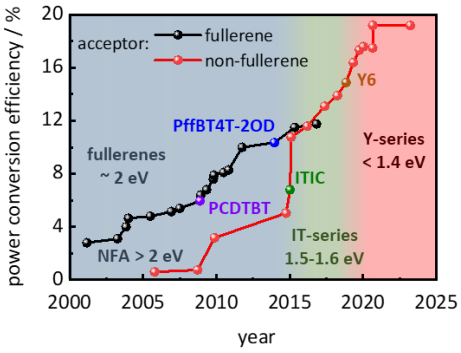

This plateauing was mainly due to the weak absorption of fullerenes in the visible to near infrared spectral range but also due to the difficulty to tune the energies of their frontier orbitals for optimization of the energy offset to the polymer donor. The situation changed with the emergence of a new class of non-fullerene acceptors, with the first prominent example being ITIC.[8] In contrast to the spherical geometry of fullerenes, this acceptor exhibits a planar fused ring donor core, end-capped on both sides with an acceptor unit. Because of its acceptor-donor-acceptor (ADA) structure, intramolecular charge transfer causes a significant red-shift of the absorption spectrum while the high stiffness and planarity of the core allow for strong intermolecular interactions. This pioneering work was the starting point for numerous chemical variations, with the goal to tune the energy levels and energy gaps of the non-fullerene acceptors to complement the properties of the donor. In 2018, Y6 was developed, yielding spectacular efficiencies exceeding 15% in combination with the donor polymer PM6.

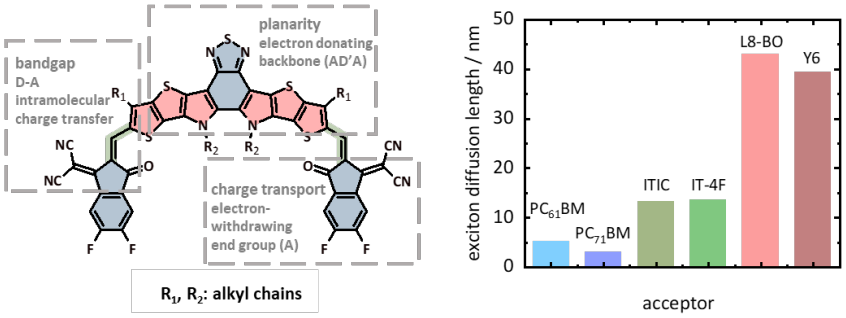

In contrast to the IT-family, acceptor molecules of the Y-series exhibit a ADA'DA chemical structure combined with a unique curved molecular shape.[8] Related to this structure is a further lowing of the energy gap as well as the ability to form multiple intermolecular interactions with the benefit of efficient exciton and charge transport.[9] In fact, these non-fullerene acceptors can show extraordinarily large diffusion lengths of up to 50 nm[10] for excitons and several hundred nanometers for charge carriers.[11] As such, the rise of the game-changing non-fullerene acceptors such as the IT-family and Y-family[12] paved the way to efficiencies of organic solar cells currently exceeding 19%.[13,14] For a more general and in-depth view on the field of non-fullerene acceptors, we kindly refer the reader to the recent literature on the subject.[15-20] For a focus on the molecular design of narrow-gap organic absorbers, the account by Cheng et al. is recommended.[21]

Organic Subcell

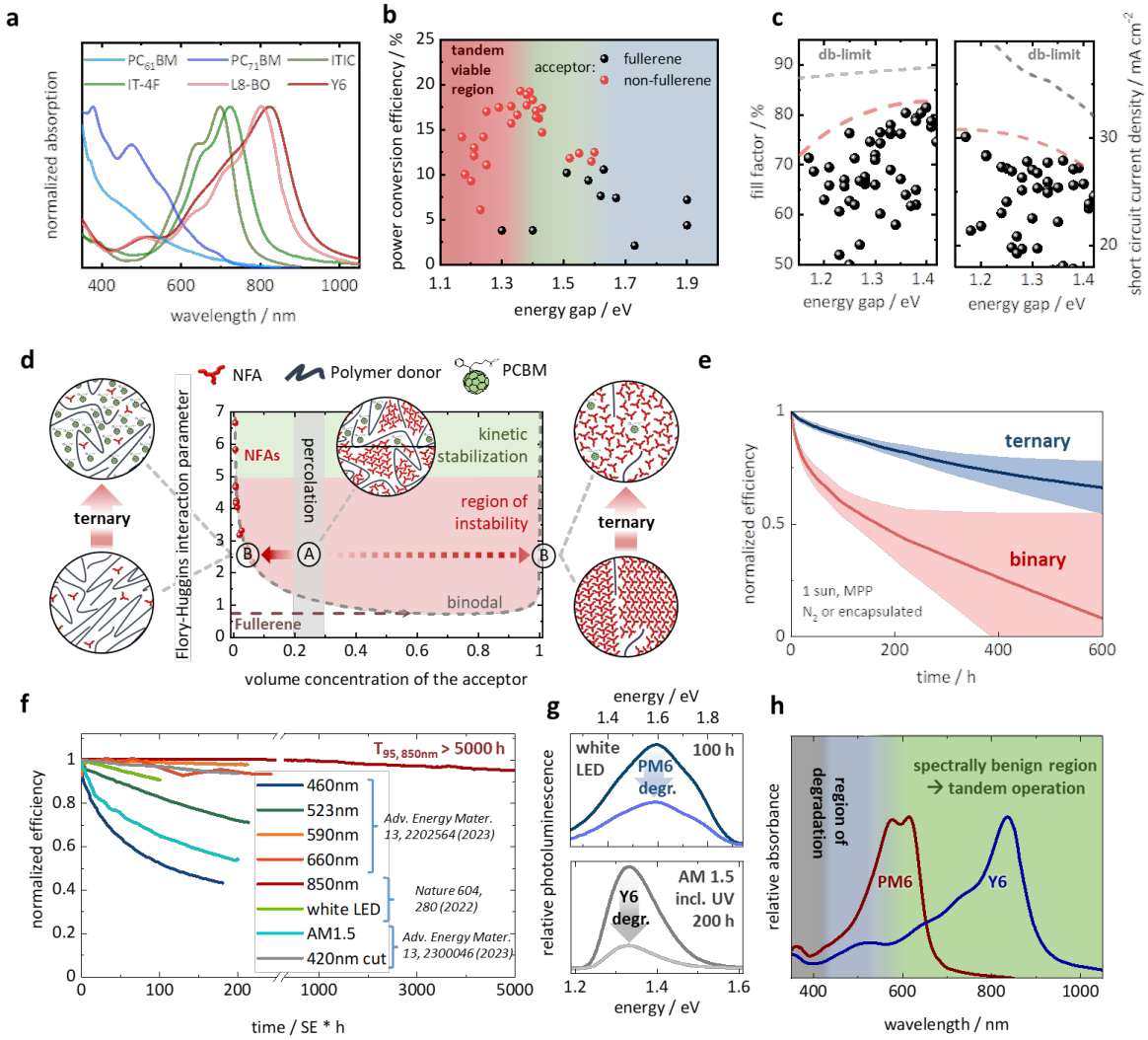

Figure 2: Organic subcell. a, *Tunable absorption spectra of non-fullerene acceptors.*[12,22,23] ***b,*** *Efficiency of organic solar cells in dependency of the optical gap of the narrow-gap constituent highlighting candidates viable for tandem application.* ***c,*** *Fill factor (left) and short circuit current density (right) of narrow energy gap non-fullerene acceptor organic solar cells in comparison to the detailed balance (db) limit. The dashed lines are a guide to the eye and highlight the increasing losses with lowering the effective energy gaps. Please note, that all energy gaps were determined from the absorption onset of the narrow-gap absorber. Open circuit voltages of and source references for the scatter plots can be found in the supporting information.* ***d,*** *Miscibility binodal (Flory-Huggins interaction parameter χ vs. acceptor volume concentration in a PM6 polymer medium of non-fullerene acceptors and the fullerene $PC_{61}BM$ that is used to form a ternary bulk-heterojunction along with a proposed mechanism of stabilization in the ternary blend. Adapted with permission from* [24] *and* [25]. ***e,*** *Comparative visualization of published stability data of binary and ternary bulk-heterojunction solar cells upon full spectrum (white LED or AM1.5, 1 sun) illumination. The lines denote the average values, the shaded areas mark the standard deviation.* ***f,*** *Operational stability of bulk-heterojunction solar cells based on PM6 and Y6 in dependency of the photon energy comprising illumination either with broadband spectra (white LED or AM1.5) or with monochromatic light sources. Data from* [4,18-20,26,27] ***g,*** *Relative photoluminescence of (top) PM6 before and after 100 h of illumination with a white LED (no ultraviolet component)*[4] *and (bottom) Y6 before and after 200 h AM1.5 irradiation (including the UV part). Note, no significant drop in PM6 was found in the same experiment.*[27] ***h,*** *Proposed critical wavelength regions for the degradation of PM6 and Y6 as well as the spectrally benign region, that enables stable operation of the organic solar cell, e.g. in a tandem application, overlayed with the respective absorbance of PM6 and Y6. Relative absorption taken from*[4]*. References sourcing c can be found in the supporting information.*

After leveling at power conversion efficiencies slightly above 10% for several years, the emergence of non-fullerene acceptors unlocked an astonishing rise of efficiencies for organic solar cells (see Box 1), that simultaneously enabled unprecedented prospects for organic solar cells in tandem architectures. The absorption onset of the non-fullerene acceptors extending well into the infrared spectral region is of key relevance in this regard (Figure 2a). While Y6 has an effective energy gap of 1.33 eV, the energy gap was further lowered to 1.21 eV by extending the donor-acceptor bridge and by modifying the chemical structure of the donor unit, which yielded short circuit current densities of more than 30 mA cm^{-2}.[28] As will become clear in the course of this perspective, for tandem architectures with organic narrow-gap subcells, a further reduction of the energy gap would be desirable.[4,29] However, as shown in Figure 2b and c, lowering the energy gap below 1.3 eV currently comes at the cost of lowered device efficiency. In contrast detailed balance (db) would suggest only a moderate variation of the efficiency between 1.1 eV and the optimum gap for single junctions of 1.3 eV. One specific feature of organic molecules is their large non-radiative losses, which lower the open circuit voltage (V_{OC}) well below the db-limit. Therefore, a higher energy gap compared to most other inorganic semiconductors is needed to realize optimum conditions with respect to the db-limit. In addition, the rate of non-radiative recombination causing this loss increases exponentially with decreasing the energy gap,[30] similar to the energy gap law of fluorescence in conjugated molecules as first proposed by Englman and Jortner in the 1970's,[31] implying that the voltage-loss becomes more severe for a smaller bandgap. Our survey of reported device characteristics of non-fullerene base organic solar cells however reveals that upon decreasing the energy gap of the absorber, also the fill factor (FF) and even more the short circuit current density (J_{SC}) lag increasingly behind the detailed balance limit (Figure 2c). As both properties are determined by the competition between free charge extraction and recombination,[32] this trend may in part be related to the increased non-radiative recombination with smaller bandgap according to the energy gap law. In addition, a sub-optimum morphology and / or the presence of barriers and interfacial recombination at the charge extraction layers may be responsible for the trend in J_{SC} and FF.[33] Clearly more experimental work is needed to be able to relate shortcomings in device performance of narrow-gap organic solar cells to fundamental limitations. This also requires the design and synthesis of novel infrared-absorbing non-fullerene acceptors, which may help to understand the efficiency limit at different energy gaps.

In addition to optimizing the efficiency of the organic solar cell, attention also must be given to its stability. In organic solar cells, both, the morphological stability of the bulk-heterojunction and the individual structural stability of the donor and acceptor moiety need attention. Regarding morphological stability, the main concern is to achieve and to stabilize the optimum blend morphology, which on the one hand ensures that all excitons reach a heterointerface within their lifetime but also warrants charge transport via percolation pathways. During operation and even upon extended shelf storage the two phases of most non-fullerene-based bulk-heterojunctions tend to segregate.[34-37] To understand the root cause of the de-mixing, one may consider the Flory-Huggins theory, where the acceptor is treated like a solvent for the donor polymer, which enables the calculation of an interaction parameter χ as a measure for their miscibility, i.e., low (high) χ indicates good (poor) miscibility.[38] χ considers the enthalpic contribution, counteracting the entropic driving force that always favors mixing.[38] A phase diagram (e.g., χ vs. the acceptor-volume-concentration (ϕ)) can be plotted, wherein a binodal curve separates the region of the single mixed phase from a system with two phases. Exemplarily, Figure 2d shows such a phase diagram for PM6 as donor.[24,39-42] To achieve optimal morphology, ϕ should be within a so-called percolation region (around 20-30% of acceptor in the donor-rich phase). Unfortunately, for many non-fullerene systems, χ is rather high (indicating poor miscibility with the donor) and thus the thermodynamically stable regions are located outside the percolation region.[25] Bulk-heterojunctions are therefore typically processed by kinetic

quenching[42] and/or the use of solvent additives (A in Figure 2d).[43-45] This approach renders the bulk-heterojunction mixture thermodynamically unstable and gives rise to a further de-mixing of the donor and acceptor molecules during operation or shelf storage into rather pure, thermodynamically more stable but with respect to the functionality of an organic solar cell unfavorable phases (B in Figure 2d).[24] Note, that de-mixing often precedes crystallization of the non-fullerene moiety. In contrast, for fullerenes such as $PC_{61}BM$ in PM6, χ has a low value of about 0.8 at room temperature (Figure 2d), indicating a good miscibility of the two components, and consequently, a rather high concentration of the fullerene acceptor in the polymer donor phase.[25] Therefore, utilizing fullerenes as third component to create a ternary blend offers an exciting opportunity to reduce morphology-related degradation of polymer:non-fullerene bulk-heterojunctions (Figure 2d).[24,46] Hereby, a typical concentration of 20 mol% fullerene mixed with the donor polymer maintains percolated pathways for electrons, while the miscibility of the fullerene with the non-fullerene acceptor will simultaneously prevent the formation of large, crystallized domains of the non-fullerene acceptor.[24,47] The applicability of this scenario to PM6 systems is supported by reports on binary PM6:$PC_{71}BM$ solar cells, that indicate efficient exciton splitting and charge transport through fullerene pathways.[48] Consequently, ternary bulk-heterojunctions reported in the literature show significantly higher operational stability than their binary counterparts (Figure 2e).

However, even a well-percolated bulk-heterojunction can only remain functional if the constituting organic molecules are themselves stable under illumination. The issue of photodegradation has been persistently accompanying the development of organic photovoltaics from the very beginning.[49-51] We want to note that both efficiency and stability of organic solar cells are critically affected by the charge extraction layers.[52] While the photo-catalytic decomposition of the organic active materials at the interface to ZnO[53,54] or the notorious stability issues associated with the use of PEDOT:PSS as hole transport layer[55] can be overcome by interface engineering, intrinsic photo-instability of the organic absorbers might be a fundamental issue. For fullerene-based organic solar cells high energy photons have been identified to cause photo bleaching.[56,57] Similar detrimental effects have also been observed for non-fullerene based organic solar cells, resulting in a substantial loss in efficiency over time, even in ternary bulk-heterojunctions and even if atmospheric influences are excluded (see Figure 2f, AM1.5). Notably, the severity of photo-induced degradation shows a distinct dependency of the illumination conditions as can be seen in Figure 2f, where the stability of PM6:Y6 systems under various spectral illumination conditions is presented.[4,26,27] While for wavelengths above 590 nm stable operation is possible, an increasingly rapid decay is found towards shorter wavelengths. Complementary photoluminescence investigations of the individual components provided further insight (see Figure 2g).[4,27] Careful interpretation of those data as a whole gives indications of two wavelength dependent degradation motifs that may partially overlap. Brinkmann et al. showed (Figure 2g, top) a substantial reduction of the photoluminescence of PM6 after prolonged irradiation with a white LED (no ultraviolet spectral components), while the emission from the Y6 acceptor was less affected by the same aging conditions.[4] In seeming contrast, Liu et al. (Figure 2g, bottom) observed a severe degradation of the Y6 acceptor upon exposure to the full AM1.5 spectrum (including ultraviolet parts), which was attributed to the cleavage of the vinylene link between the core and the acceptor due to the spectral components below 420 nm. At the same time, the PM6 appeared to be less affected.[27] In the same study, application of an ultraviolet cutoff filter drastically improved the long-term stability (Figure 2f). The spectral range up to 590 nm on the other hand appears more detrimental for the stability of the PM6. Note, a white LED operated at one sun equivalent intensity contains a higher amount of such supposably critical photons in the range between 420-590 nm compared to the broadband AM1.5 spectrum and it will therefore cause more severe degradation of the PM6 polymer. A possible mechanism of PM6 degradation is the photo-induced dihedral twisting of the PM6 chains around the

benzo[1,2-b:4,5-b']dithiophene-thiophene link. Twisted chains may allow for a closer contact between donor and acceptor unit of neighboring chains and are suspected to mediated singlet exciton to interchain polaron pairs and further trap-mediated non-radiative recombination.[58] While this twisting was found to be accelerated in the presence of oxygen and moisture, the authors reasoned that the process would likewise occur under inert conditions. Upon irradiation in the spectral range below about 420 nm, though Y6 degradation is more pronounced, both PM6 and Y6 are expected to degrade.

In any event, in a tandem architecture the light reaching the organic subcell will be filtered by the wide-gap perovskite positioned in front (see Figure 1a). As such, the organic cell is expected to be operated exclusively in the spectrally benign region highlighted in Figure 2h, where already encouraging operation stabilities exceeding 5000 hours have been shown.[4] For further optimization, new efficient acceptor materials need to be developed, that enable even lower absorption onsets while maintaining a high J_{SC} and FF. Thereby, not only a higher J_{sc} and an improved overall performance of the tandem cell can be achieved but at the same time the bandgap of the perovskite absorber can be lowered, which will also positively impact on the operational stability of the perovskite subcell, as discussed in more detail below.

Perovskite Subcell

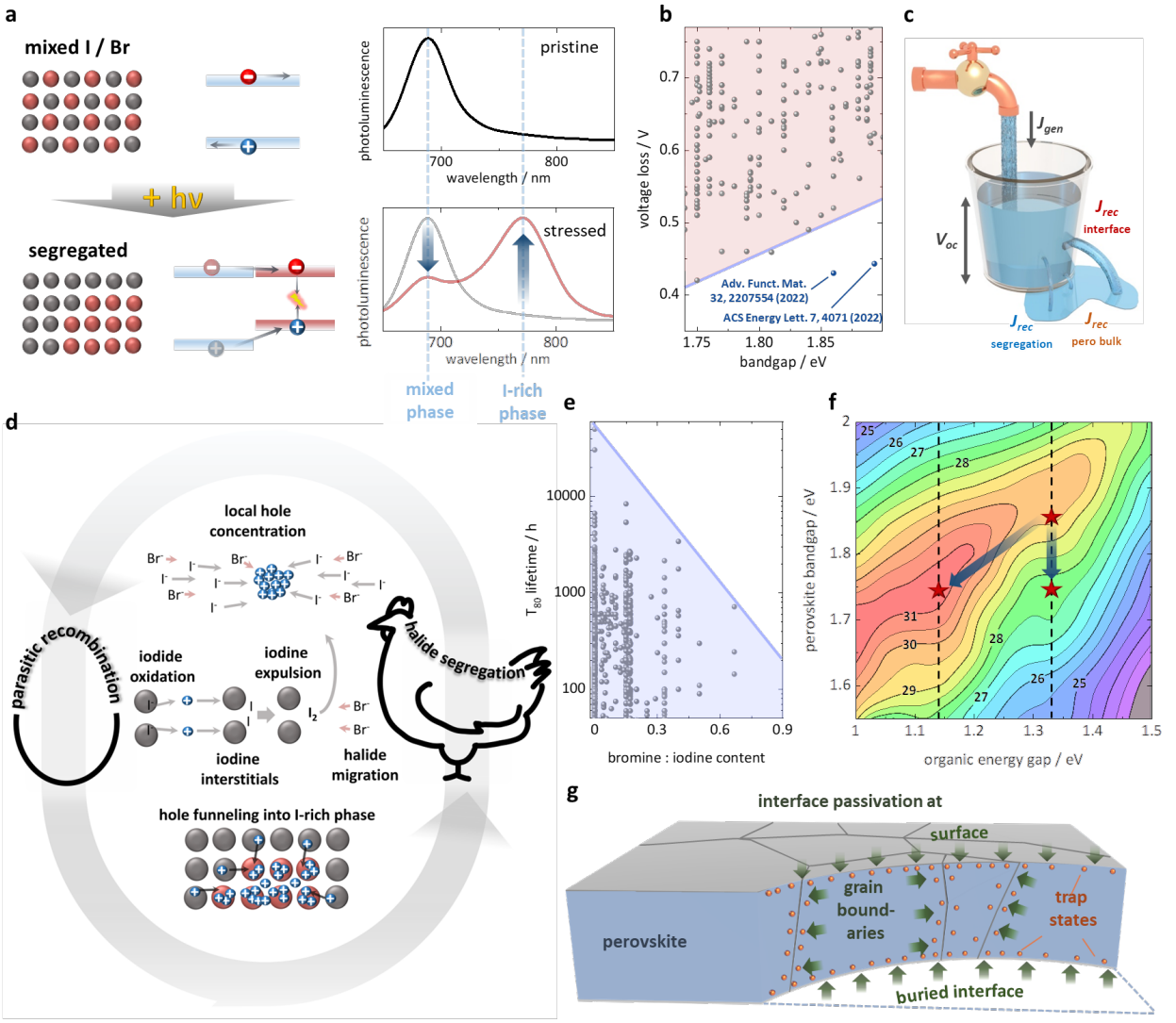

Figure 3: Challenges and perspectives of wide-gap perovskite cells for tandem application. a, *Schematic illustration of the process of illumination triggered halide segregation with energy level diagram and measured photoluminescence of (top) the pristine, mixed phase and (bottom) the light-stressed, segregated phase. Photoluminescence shown in a, taken from*[4] ***b,*** *Literature survey for open circuit voltage-loss of perovskite solar cells in dependence of the perovskite bandgap* ***c,*** *Bucket model of recombination losses limiting the open circuit voltage of the wide-gap perovskite solar cells highlighting the crucial role of interface recombination.* ***d,*** *Hen and egg analogy connecting halide segregation to parasitic recombination (e.g., at interfaces, grain boundaries) encasing proposed mechanisms that cause or further halide segregation. Grey and red spheres represent mixed and segregated sections of the perovskite lattice.* ***e,*** *Overview of T_{80} stability under illumination reported in literature in dependence of the iodine:bromine ratio.* ***f,*** *Heat map displaying the potential of perovskite-organic tandem solar cells assuming an optimistic, yet realistic scenario of a voltage-loss of 0.4 V and a tandem fill factor of 85%. Please note that these considerations are made using measured optical data shifted on the energy axes, which is why they present a realistic scenario. For details see ref* [4]*. The stars depict the current position of record tandem cells and the perspective of reducing the perovskite bandgap both with and without concomitant reduction of the organic solar cell's energy gap. Adapted with permission from* [4]*.* ***g,*** *Schematic illustration of interface trap state passivation. The references sourcing b and e can be found in the supporting information.*

The optimal choice for the wide-gap perovskite subcell material, is determined by the bandgap of the narrow-gap organic solar cell. Highly efficient perovskite-organic tandem solar cells reported, so far, primarily rely on the PM6:Y6 system, which, according to optical simulations, is ideally paired with a perovskite solar cell having a bandgap around 1.85 eV.[4] A general overview of wide-gap perovskite solar

cells is provided by dedicated review articles on the matter.[59-61] In this perspective we will focus on the notorious phase segregation in wide-gap perovskite cells, which represents the most pressing bottleneck for the stability of perovskite-organic tandem solar cells (see Table S6).[62]

The bandgap of halide perovskites can be tuned by variation of the halide, whereby a bandgap of 1.85 eV requires a mix of iodine and bromine in the range of 1:1. Unfortunately, at elevated bromine:iodine ratios the perovskite phases tend to segregate into iodine-rich and bromine-rich domains upon illumination (see Figure 3a).[63-65] Halide segregation is regularly accompanied by an apparent deficit in V_{OC} (Figure 3b), that compromises cell performance and one might intuitively link this loss with recombination caused by funneling charges to the more iodine-rich regions. However, attempts to model the deficit resulting from halide segregation due to increased radiative recombination in the iodine-rich regions have concluded that it can only account for approximately 20% of the observed recombination losses (Figure 3c).[66] A way to quantify the loss from halide segregation is to track the evolution of the photoluminescence emission from the mixed phase (Figure 3a).[67] If most carriers funnel into the iodine-rich domains (see Figure 3a, bottom), the quasi-Fermi-level splitting of the mixed phase will be reduced as will be the achievable V_{OC}. Segregation however may be identified in photoluminescence even at a very early stage, because of the high radiative efficiency due to confinement of charges in the segregated phase.[67] In this case, halide segregation will not infer a significant penalty on the voltage, rather losses in current density caused by ion induced field screening have been evidenced recently.[68] Indeed, direct evidence confirms a significant reduction of quasi-Fermi-level splitting is due to recombination at the interfaces of non-segregated perovskite phases and adjacent charge transport layers rather than due to halide segregation.[69] As a result, substantial advancements in perovskite-based tandem solar cells have been achieved by reducing voltage-losses through suppression of interfacial recombination in wide-gap perovskite solar cells.[4,6,70-74] Two remarkable examples of successful interface optimization are highlighted in Figure 3b. Reported efficiencies for wide-gap perovskite single junctions (e.g., with a bandgap of 1.79 eV) exceed 20 %, today.[72]

Aside from efficiency considerations, minimizing halide segregation has important implications for the stability of the device. Although halide segregation generally is a reversible phenomenon due to entropy-driven redistribution of halide anions,[63,75-77] illumination-driven diffusion of halides out of the perovskite layer and into the charge transport layers or electrode interfaces can ultimately lead to irreversible degradation.[78-81] Figure 3e displays a correlation between increasing bromine content in mixed halide perovskite solar cells and lower solar cell lifetime. Despite the prevalence of halide segregation in perovskite absorber layers, the underlying mechanism is still not well understood. The observed phenomena are inherently complex and likely depend on film deposition conditions and stressing conditions such as the spectral characteristics and intensity of illumination or the experimental environment. Proposed models to explain halide segregation encompass a range of factors, including thermodynamics, lattice strain, carrier concentration gradients, electrical fields caused by trapped holes and crystallographic phase instability.[65,76,82-85] However, there is currently no model that unambiguously explains the full range of experimental observations, including temperature dependencies, threshold illumination intensity, stationary composition, field dependence, re-mixing, cation dependency and more.[64,76,83,86] Experimental evidence anyhow strongly suggests a link between halide segregation and an increased parasitic recombination (such recombination that doesn't convert optical to electrical power).[4,64,67,82,87] Nevertheless, the causality between halide segregation and parasitic recombination remains uncertain, leading to a "hen-and-egg" situation, as both could potentially be the root cause of the other (Figure 3d). Compelling evidence indicates that halide segregation and subsequent device degradation are driven by localized positive charges, such as an excess accumulation of holes at local trap

sites or in the segregated iodine-rich phase.[68,77,84,88-90] Additionally, oxidation of iodide sites from photogenerated or injected holes, resulting in weakened Pb-I bonds has been observed.[82,91-93] Expulsion of such oxidized species from the lattice, might create interstitial defects that act as trap states and halide vacancies, that further halide migration.[77] The critical role of holes is further supported by an apparent dependency of halide segregation on electrical fields, even in the absence of illumination.[82,94] On the other hand, iodine-rich regions in general act as localized traps for holes, as the band gap reduction is primarily driven by the valence band.[88,95,96] Yet, mixed halide films are not necessarily perfectly uniformly mixed initially. Nanoscale compositional heterogeneity has been demonstrated in the initial mixed-halide films, that may initiate the phase separation on the macroscale while simultaneously acting as recombination sites.[97,98] Thus the "Hen-and-Egg" situation remains unresolved to date.

Given the promising stability of organic solar cells discussed above, the wide-gap perovskite remains the bottleneck for stability of perovskite-organic tandem solar cells (see Table S6). In a tandem architecture, halide segregation even complicates cell characterization. Light biasing that is needed for the measurement of the external quantum efficiency of the subcells constitutes a strongly asymmetric stress, that, due to current mismatch, leads to carrier accumulation and eventually degradation.[4] As the characterization of subcell quantum efficiency is typically required in a certification procedure, the certified and in-house efficiency values currently show substantial deviations (for example 23.1 % vs 24 %,[4] or 22.9 % vs. 23.6 %[6]). Perovskites with a narrower bandgap, and therefore increased operational stability, would become feasible for integration in tandem devices, if the absorption onset of the organic subcell could be further reduced (Figure 3f). Accordingly, both efficiency and stability of perovskite-organic tandems could benefit from progress in the field of narrow-gap organic solar cells, with a realistic efficiency potential reaching well beyond 31%. Note, calculations based on the detailed balance limit only, result in efficiencies as high as 45%.[15]

To address halide segregation, various strategies are being employed, which are focused mostly either on reducing inhomogeneity, strain or trap density in the bulk perovskite phase or preventing hole accumulation at interfaces.[64] The improvement of bulk properties often involves modifying the crystallization process or adjusting the perovskite composition. Among others, additives, modified annealing conditions, non-stoichiometric solutions, process engineering, A-cation tuning, incorporating 2D/3D structures or crystallization agents have yielded retarded halide segregation.[61,65,73,98-103] In addition, strategies to mitigate interface hole accumulation range from tailored charge extraction layers such as self-assembled monolayers, passivation agents at the perovskite surface or grain boundaries, to low dimensional perovskite capping layers, aiming to prevent trap formation (Figure 3g).[4,104-106] For general reading on interface engineering for perovskite solar cells, the reader is kindly referred to the literature.[107] Another approach might be to use all-inorganic perovskites. All-inorganic perovskites, such as $CsPb(I_{1-x}Br_x)_3$, can provide a bandgap of 1.7 eV with a relative bromine content below 20% in while a relative bromine content of about 25-30% is needed with organic cations to achieve the same bandgap.[108-110] Here, increased stability can be expected not only due to the reduced tendency for halide segregation, but also due to a generally higher resilience against thermal or illumination stress.[111-114] The sensitivity of these perovskites against ambient air[115] can be likely mitigated by proper encapsulation. Additionally, all-inorganic wide-gap perovskite solar cells typically rely on an n-i-p architecture, which necessitates an adaption of the entire tandem cell (including the organic subcell). Stability issues in n-i-p organic solar cells, that are associated with the choice of electron transport material, need to be taken into account in this case.[53,54] Another strategy might be the incorporation of a large dimethylammonium cation into pure iodide perovskites with a high Cs-ratio, which has been shown to widen the bandgap and

stabilize the perovskite absorber.[116] Highly efficient Br-free perovskite solar cells with bandgaps relevant for the application in perovskite-organic tandem solar cells are yet to be demonstrated.

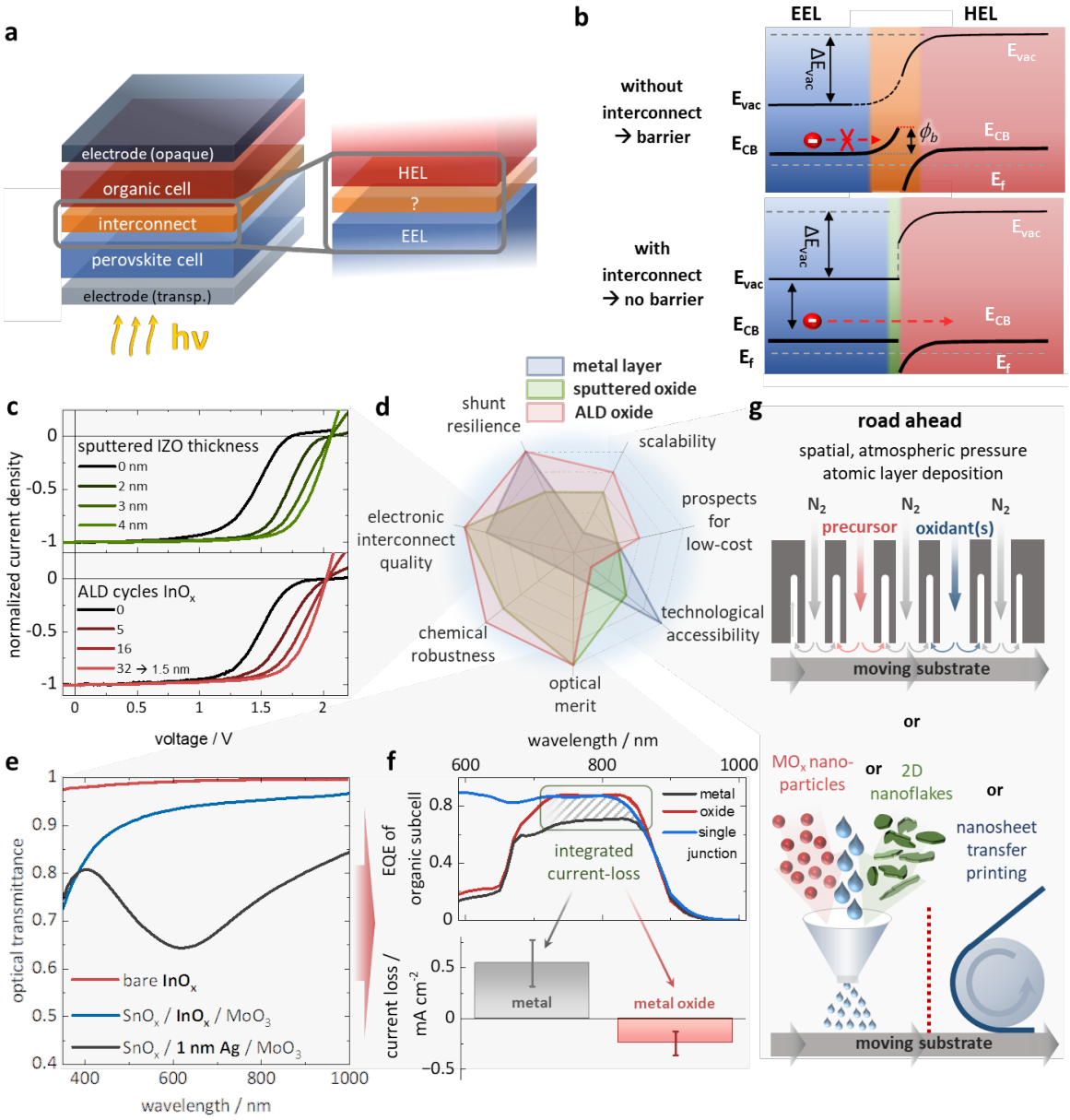

Figure 4: The interconnect in perovskite-organic tandem solar cells. a, *Solar cell stack of a perovskite-organic tandem solar cell with a spotlight on the interconnect between the electron extraction layer (EEL) of the perovskite solar cell and the hole extraction layer (HEL) of the organic solar cell.* ***b,*** *Energetic line-up of the EEL / HEL interface both without (top) and with (bottom) a recombination interconnect. Adapted with permission from [4].* ***c,*** *J-V characteristics of perovskite-organic tandem solar cells employing different thicknesses of metal oxide interconnects. Adapted with permission from [4,6].* ***d,*** *Radar chart qualitatively evaluating the properties and prospects of metal and metal oxide interconnects with respect to various technical and economic aspects.* ***e,*** *Optical transmittance of the metal oxide interconnect bare and sandwiched between charge extraction layers in comparison to an evaporated silver interconnect. Adapted with permission from [4].* ***f,*** *(top) External quantum efficiency (EQE) data exemplarily comparing the current-loss in the organic subcell caused by the interconnecting layers with respect to the single junction.[4] (bottom) Integrated current density loss derived from EQE data (integrated between 720-830 nm excluding the perovskite or organic absorption onset) of either metal oxide or metal interconnects reported for perovskite-organic tandem solar cells.* ***g,*** *The road ahead for tandem interconnects depicting the concept of spatial atomic layer deposition (top) and alternative roll-to-roll deposited (bottom), ultra-thin interconnects consisting of either metal oxide nanocrystals or two-dimensional materials via solvent or dry-transfer processes. The references sourcing f can be found in the supporting information.*

Interconnect

In monolithic tandem solar cells, an interconnect is needed, that facilitates the electronic connection between the subcells. In the following we focus our discussion on p-i-n type solar cells (Figure 4a), as the most efficient perovskite-organic tandem cells currently employ this architecture. Here, the interconnect joins the electron extraction layer of the perovskite wide-gap subcell with the hole extraction layer of the narrow-gap organic subcell, that is typically processed on top. In general, an interconnect must fulfill three main requirements: 1.) Transfer of charges between the two subcells, ideally without any V_{OC}-loss while maintaining a high FF. 2.) Optical transparency to avoid losses in J_{SC} of the back-cell. 3.) Mechanical/chemical shielding to protect the bottom subcell from the subsequent deposition steps.

While in classical III-V multijunction cells the interconnect consists of an epitaxially grown highly doped p-n tunnel junction,[117] many thin-film tandem cells employ an n-n type interconnect architecture. For example, most highly efficient perovskite-organic tandem cells rely on an interface of a n-type electron extraction layer (EEL), such as SnO_x and an n-type hole extraction layer (HEL), such as MoO_x. Note, very efficient hole extraction by the high work function MoO_x occurs due to recombination of photo-generated holes in the highest occupied molecular orbital (HOMO) of the organic material with electrons in the conduction band of MoO_x.[118,119] In a SnO_x/MoO_x junction, photogenerated electrons from the perovskite subcell need to be handed over from the conduction band of the SnO_x to the conduction band of the MoO_x to recombine with the photo-generated holes from the organic subcell.[118-120] There is however a large difference in work function between the electron and hole extraction layer, that in case of SnO_x/MoO_x junctions results in the formation of a Schottky barrier (ϕ_b) as high as 0.6 eV (Figure 4b, top).[4]

As shown in Figure 4c, such a Schottky barrier leads to unfavorable S-shaped current-voltage characteristics of the tandem cell.[4,6] The most obvious remedy for this issue would be electrical doping of the metal oxides, as the barrier width scales as $n_e^{-½}$, where n_e is the doping density. At sufficiently high n_e the barrier would become thin enough to allow for tunneling as an efficient transport mechanism. Unfortunately, electrical doping of SnO_x typically requires elevated growth temperatures (exceeding 150°C) and the use of ozone or oxygen plasma processes, which is not compatible with the deposition on top of a perovskite.[121,122] Therefore, an additional layer with a high n_e is inserted between the subcells that forms an ohmic contact to SnO_x and concomitantly establishes an interface with a narrow barrier to the MoO_x (Figure 5b, bottom). Specifically, ultra-thin metals or metal-like metal oxides with charge carrier densities above 10^{20} cm^{-3} are used for this purpose. Among the metal oxides, indium oxide is a promising candidate, that provides a high carrier density even at low processing temperatures (below 80 °C), either by intentional doping with heteroatoms, such as zinc, to form indium zinc oxide (IZO)[123] or by a self-doping effect due to oxygen vacancies.[124] Figure 4c shows the change in J-V characteristics of perovskite-organic tandem devices, with increasing the nominal thickness of two such indium oxide-based interconnects; the S-kink gradually disappears, ultimately resulting in a high FF of the tandem. Please note that similar considerations apply if instead of the n-type MoO_x a p-type material, such as PEDOT:PSS, is used.[74] It is important to note that both the choice of material as well as the deposition technique affect the nucleation and growth, and thereby the required layer thickness at which a functional interconnect is formed. For example, sputtered indium zinc oxide interconnects typically require a thickness of more than 4 nm, while indium oxide (InO_x) prepared by atomic layer deposition yields a homogeneous, continuous interconnection layer with well-behaved J-V characteristics already at a thickness of 1.5 nm.[4] For metal interconnects, typically thermally evaporated Ag or Au is used with an equivalent layer thickness in the range of 0.5-1 nm. Thin metals layers typically form islands rather than percolated thin films, which is why the statement of a film thickness is rather a measure for the mass of the deposited material resulting from

a reading of the quartz film thickness monitor. One can speculate, that the island growth of thin metal films sets a lower limit to the amount of material that is needed to render the interconnect fully functional.[125-129] We want to point out, that for n-i-p structured all-organic tandem devices, highly performing all-oxide interconnects based on MoO_3/ALD-SnO_x or MoO_3/ALD-ZnO have been reported.[120] Interestingly all current n-i-p type perovskite-organic tandem solar cells solely rely on metal interconnects, that are known to infer optical losses.[70,130,131] We anticipate that the field of n-i-p type perovskite-organic tandems would tremendously benefit from the use of low-loss all-oxide interconnects. Potential stability issues caused by a MoO_3 hole extraction layer could be addressed by substitution with vanadium oxide,[132] which was shown to provide similar electronic properties and improved thermal stability.[119,133]

The thickness of the interconnect is an important parameter, since it affects two important aspects, both of which are crucial for the functionality of the tandem solar cell. On the one hand, a thin layer typically results in high sheet resistance, which is highly beneficial for an interconnect as it prevents the connection of possible shunt paths in the individual subcells and thereby renders shunting of the tandem cell less likely.[134] In this regard, non-percolated metal layers and ultra-thin indium oxide layers grown by atomic layer deposition offer advantages over thicker and more conductive indium zinc oxide layers. On the other hand, a low optical absorbance is essential to minimize optical losses.[114] While indium oxide-based interconnects are transparent over a wide spectral range, even ultra-thin metal films infer significant optical losses (Figure 4e).[4] This loss in transmittance severely lowers the external quantum efficiency of the narrow-gap subcell. In contrast, the use of a metal oxide as an interconnecting layer enables an external quantum efficiency of the back cell, that essentially resembles that of the single junction (Figure **4**f). A slight increase in some spectral regions might be related to beneficial optical effects. Integrated current-loss between the single junction and the tandem subcell in the spectral region of 720-830 nm demonstrates the superiority of the metal oxide interconnect (Figure 4f, bottom). We want to note a report of a C_{60} / tin oxide (SnO_x) interconnect, that utilizes an ambipolar SnO_x (x = 1.76), layer, where a high density of mid-gap states in tin oxide is claimed to account for hole transport capability.[135] However, as oxygen deficiency in metal-oxides frequently infers optical absorption, it remains to be shown if this strategy is generally applicable to further reduce optical losses compared to interconnects based on ultra-thin indium oxide. For chemical robustness anyhow, a metal oxide, such as tin oxide grown by atomic layer deposition, is often used underneath the interconnect. Tin oxide can form dense and pinhole-free layers that provide remarkable resilience against harmful solvents and offers excellent properties as permeation barrier.[78,121,122,136,137] In addition, metal oxides also have the advantage of chemical durability, as metal layers tend to react with perovskite constituents if not properly shielded.[79,138] Although currently (in)stability of perovskite-organic tandem cells is primarily governed by halide segregation in the wide-gap perovskite, the degradation of metals within the device may likewise become a serious bottleneck.

It can be concluded that ultra-thin metal oxides as interconnects exhibit nearly optimal properties in terms of optical and electrical functionality. Further progress regarding the efficiency of perovskite-organic tandem solar cells will therefore most likely originate from improvements of the two subcells (even if a non-ideal interconnect is used). However, scalability and accessibility remain critical challenges. Homogeneous coating of large area substrates with sub-nm thickness-control by thermal evaporation or sputter deposition is challenging.[139] On the other hand, atomic layer deposition has been shown to be compatible with roll-to-roll processing through the use of the so-called spatial atomic layer deposition (Figure 4g, top), that can even be operated at atmospheric pressure, as demonstrated for tin oxide in perovskite solar cells.[122,136,140] Unfortunately, the spatial atomic layer deposition of InO_x requires relatively harsh process conditions, such as high temperatures (above 150 °C) and oxygen plasma.[141-143] Therefore,

the growth of indium oxide interconnects by spatial atomic layer deposition under mild conditions, as required for perovskite-organic tandem solar cells,[4] has yet to be demonstrated. With respect to accessibility and prospective low-cost manufacturing, it may be attractive for the scientific community to explore alternative methods to deposit extremely thin transparent materials with high charge carrier density. Several promising approaches could be considered, including print- or spray-deposited metal oxide nano-particles[144,145] or high carrier density 2D materials.[146]

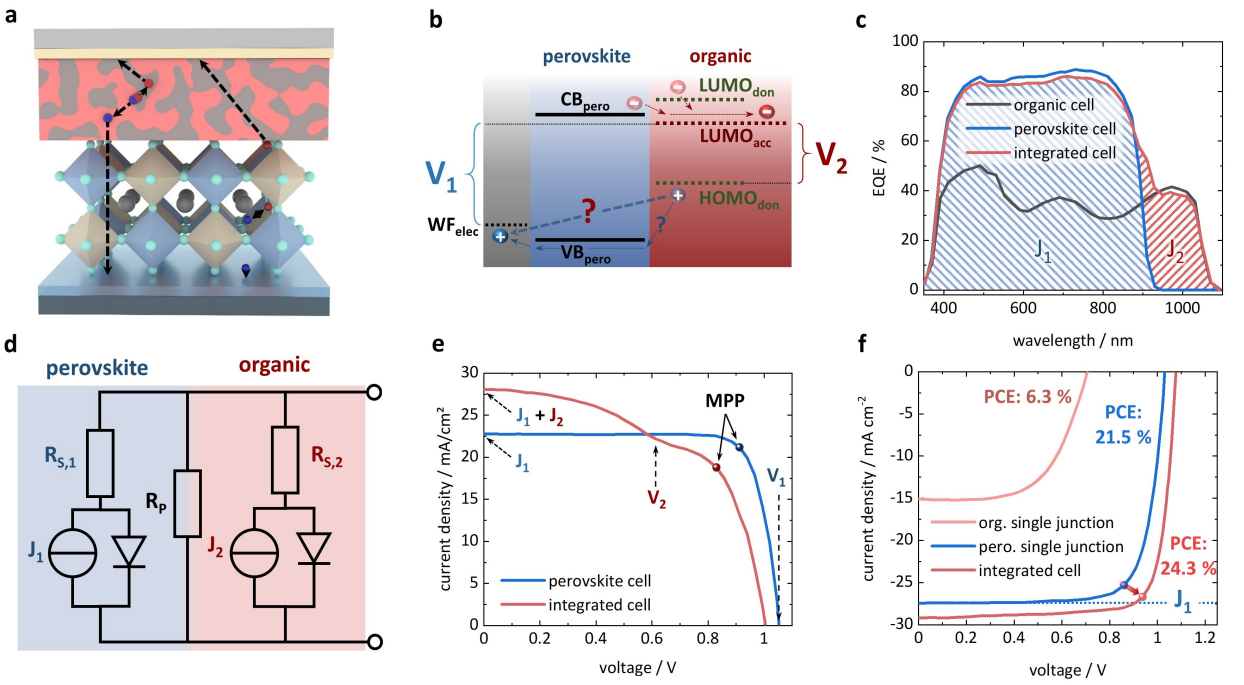

Figure 5: Integrated perovskite-organic solar cells. a, *Schematic illustration of the setup of an integrated solar cell also showing the proposed transport path of generated charge carriers.* ***b,*** *Energy level diagram (omitting potential interface effects and band bending) that illustrates possible transitions for charge transport between the perovskite and the organic bulk-heterojunction. V_1 and V_2 depict the open circuit voltage potentials of the perovskite (V_1) and the bulk-heterojunction (V_2).* ***c,*** *External quantum efficiency (EQE) of an exemplary perovskite, organic and integrated solar cell. J_1 represents the short circuit current density of the perovskite single junction, J_2 the extension of the EQE spectrum by the bulk-heterojunction. Adapted with permission from [147].* ***d,*** *Equivalent circuit model using a parallel connection of two one diode models to display the supposed operation principle of integrated perovskite-organic cells. The diodes D_1 and D_2 model the two different potentials of generated charge carriers (see b), while J_1 and J_2 the current density contribution of the perovskite (J_1) and the EQE extension by the bulk-heterojunction (J_2). $R_{s,1}$ and $R_{s,2}$ model the respective transport resistances for generated charge carriers and R_p the overall shunt resistance of the whole integrated device.* ***e,*** *J-V characteristics showing a published example for the effect of the parallel connection on the solar cell characteristics. The respective influence of the individual current densities and voltages from b-d (J_1, J_2, V_1, V_2) are highlighted as well as the position of the respective maximum power point (MPP). Adapted with permission from [148].* ***f,*** *Best so far published integrated perovskite-organic solar cell. The shift of the MPP is highlighted as well as the J_1 showcasing the compliance with the $J_{MPP} \leq J_1$ requirement of a parallel connection. Adapted with permission from [147].*

Integrated Perovskite-Organic Solar Cells

There are numerous reports on so-called "integrated" perovskite-organic solar cells, which are sometimes considered an alternative approach to realizing a perovskite-organic tandem cell without the need for an interconnection layer.[149-153] In these devices, the organic bulk-heterojunction is directly positioned on top of the perovskite material, as shown in Figure 5a. To provide some clarity regarding their functionality and nomenclature, these integrated solar cells will also be briefly discussed here.

Firstly, to understand the operation principle of these integrated cells, it is important to note that most of the utilized bulk-heterojunctions contain $PC_{61}BM$ as an acceptor and/or third component in a ternary blend. Assuming proper percolation, the bulk-heterojunction can therefore function as electron extraction layer for the perovskite absorber through $PC_{61}BM$ pathways.[154-156] The crux is, however, the extraction of holes from the bulk-heterojunction, which is hindered by a barrier to the valence band of the perovskite material (Figure 5b). Investigations on such integrated devices estimate an energy barrier of approximately 250 meV.[151] In short-circuit conditions, such an energy barrier can be overcome by internal electrical fields present in the device due to charge separation. J_{SC} can therefore be the sum of the current densities

produced by both the perovskite (J_1) and the bulk-heterojunction (J_2) (Figure 5c). Since not voltage, but current is additive in this configuration, a simplified parallel connection equivalent circuit model (Figure **5**d) can be applied, where the series resistors $R_{S,1}$ and $R_{S,2}$ represent the respective transport resistances for charge carriers passing through the other absorber material. To complete the picture, it is important to consider that the energies of the electron-hole pairs created in the subcells don't match. Therefore, the diodes in Figure 5d have different forward voltages (V_1 and V_2 in Figure 5b). In an open-circuit scenario, if $R_{S,1}$ is sufficiently high compared to R_p this situation does not necessarily result in a voltage limitation by V_2, as one might intuitively expect in a parallel connection. Thus, such integrated solar cells can simultaneously show increased J_{SC} ($J_1 + J_2$) and an almost unaffected V_{OC} (= V_1) (see Figure 5e). These apparent benefits however cannot be translated into the maximum power point of the solar cell. Since the electron-hole pairs created in the bulk-heterojunction have a lower energy than those created in the wide-gap perovskite absorber, they are unable to contribute to the current density at higher voltages. Consequently, the maximum power point shifts in an unfortunate manner, and the current-voltage characteristics exhibit either a severe S-shape or a shunt-like behavior (Figure 5e).[148] In numerous reports on integrated perovskite-organic cells therefore the actual power output either decreases or remains basically unchanged upon the addition of a bulk-heterojunction.[148,154,155,157,158]

Nevertheless, there are reports, in which the efficiency of perovskite solar cells improves by adding a bulk-heterojunction directly on top.[147,159-161] It is important to exercise caution however, when interpreting such data, as the improved device parameters may not necessarily result from the observed extension of the spectral response. Studies have shown that the addition of a bulk-heterojunction, instead of a simple fullerene layer, can passivate traps and reduce interface recombination.[159] Recent reports have also demonstrated that photodoping through exciton splitting in the charge transport layers can significantly enhance charge extraction.[162] Indeed, the latter report provides evidence of a remarkable increase in device performance through the addition of a bulk-heterojunction, resulting in improvements in FF, V_{OC} and even J_{SC}, without extending the spectral response. Therefore, when evaluating the actual benefits originating from spectral extension, it is necessary to disentangle them from the improvements made to the single junction performance, which is very challenging. For instance, in some of the best performing integrated solar cells, an elevated V_{OC} was recorded (Figure 5f), while the current density at the maximum power point remained significantly below the J_{SC} of the corresponding individual perovskite cell.[147,161] These observations could indicate charge extraction and interface passivation as origin for the improved efficiency, as reported by Wang et al.[162] Other reports discuss additional additive engineering of the perovskite active material[160] or atypical variations in FF,[159] all of which hinder a clear correlation between spectral expansion and efficiency enhancement. In light of the discussion above we conclude, that the concept of an integrated solar cell is most likely not viable to overcome the detailed balance limit and should not be considered a tandem technology. Rather utilization of an organic heterojunction can play a role in optimizing charge extraction and transport in perovskite single junctions.

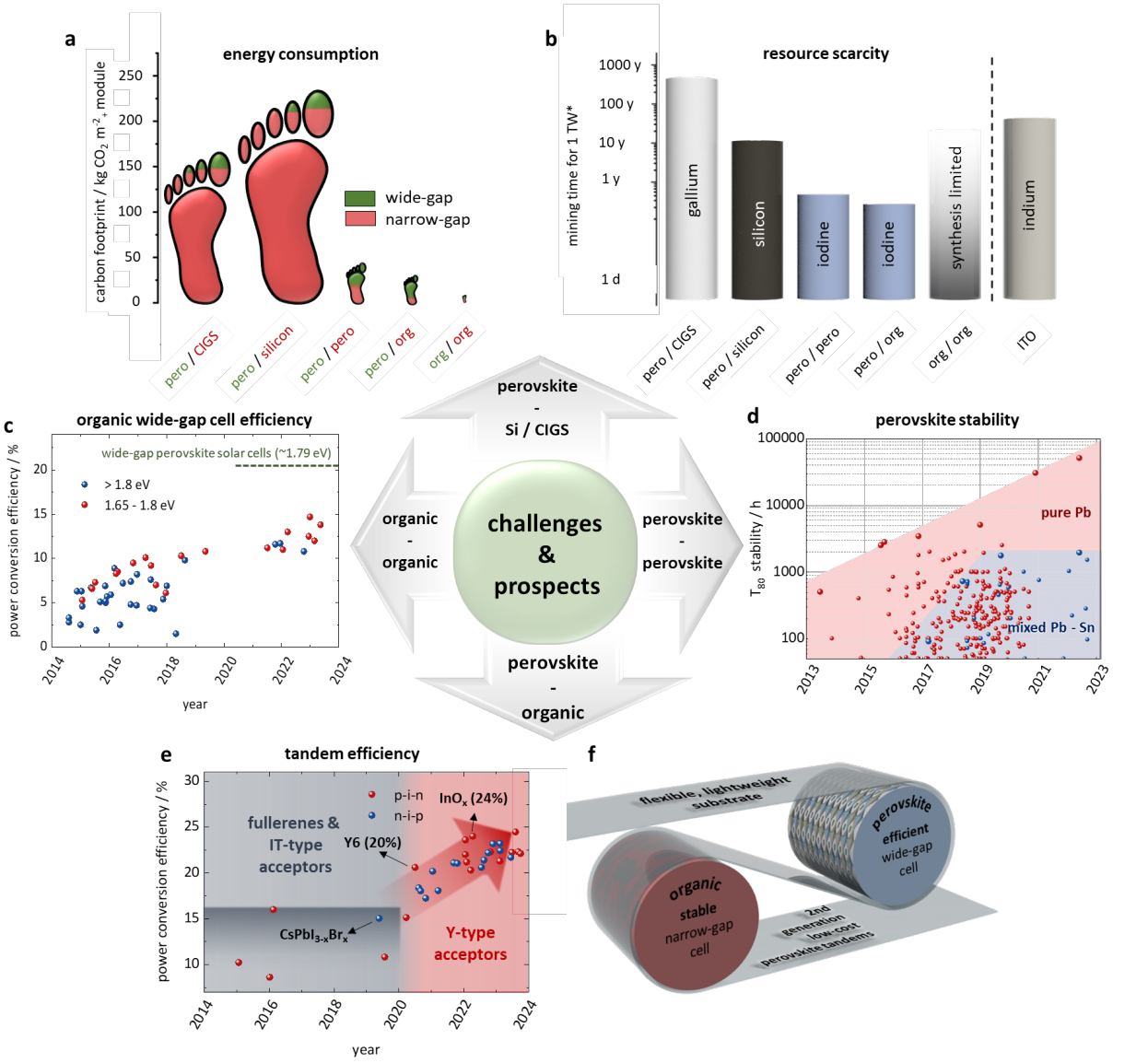

Figure 6: Perovskite-organic vs. other emerging tandem solar cells. a, *Carbon footprint of perovskite-silicon and perovskite-CIGS tandem solar cells compared to all-perovskite all-organic and perovskite-organic tandem solar cells.* ***b,*** *Resource availability (expressed by the expected time period required to mine 1 TW worth of raw material) of the critical elements required for solar technologies. Calculation for a, and b, according to supplementary note 2 from sources [163-165].* ***c,*** *Development of wide-gap organic solar cell efficiencies over the past years.* ***d,*** *Development of T_{80} operation stability of lead and lead-tin mixed metal halide perovskite solar cells under 1 sun equivalent illumination showing the apparent leveling of Pb-Sn solar cell stability. For further details please see Table S9.* ***e,*** *Power conversion efficiency development of perovskite-organic solar cells over the past 10 years highlighting the introduction of the Y-type acceptors.* ***f,*** *Illustration showcasing the potential of roll-to-roll compatible, flexible, low-cost and lightweight perovskite-organic tandem solar cells combining the strengths of both perovskite and organic solar cell technology. References sourcing c, d, and e, can be found in the supporting information.*

Perovskite-Organic vs. Other Emerging Tandem Solar Cells

To benchmark the perovskite-organic tandem technology, it is important to discuss other emerging tandem technologies and to identify their potential challenges and limitations. Perovskite-silicon tandems with their impressive efficiencies, already exceeding 33%, can be expected to become the first generation of perovskite-based tandems to enter the market.[1] An alternative approach to pair perovskite with a commercially available narrow-gap absorber is copper-indium-gallium-selenide (CIGS). While both, silicon

and CIGS are mature technologies with decades of research and development, they also face fundamental limitations like high energy consumption and/or limited availability of elements. Specifically, Silicon technology requires a high thermal budget, which leads to a comparatively long energy payback time and a substantial CO_2 footprint (Figure 6a).[163] On the other hand, CIGS faces challenges regarding the limited abundance of gallium. At the current mining speed, it would take more than 100 years to obtain the raw material exclusively for one terawatt of CIGS modules (Figure 6b). At the same time, the Gallium demand in the existing semiconductor industry (e.g., for light emitting diodes, etc.) is already critically high.[166]

In contrast, tandem technologies relying solely on perovskite and organic solar cells can overcome these challenges by utilizing abundant elements and low-temperature high-throughput processing. It should be noted that most reported perovskite and organic solar cells use indium tin oxide as transparent electrodes, which are subject to the notorious scarcity of indium.[166] Fortunately, there are numerous alternative semitransparent electrodes reported for both technologies.[121,138,167,168] A further paradigm frequently linked to perovskite and organic solar cells is the prospect of becoming lightweight and potentially flexible, thereby unlocking diverse applications beyond traditional rooftops. Facades, fences, agri-photovoltaics, and mobile applications are just some of the targeted fields, where established solar cells are typically not viable. Therefore, the second generation of perovskite-based tandem technologies to enter the market might well be a complement rather than a competitor to the perovskite-silicon technology. As highly efficient, lightweight solar technologies, both perovskite and organic solar cells have shown remarkable radiation tolerance.[169] Thus, applications in space state another highly promising complementary market for perovskite-organic tandem cells.

Still, the question remains, which combination of emerging technologies will turn out as the most promising one. Combinations of similar solar technologies might initially seem preferential, as they allow for conceptual synergies and the utilization of the same fabrication facilities for both subcells. For organic-organic tandem solar cells, the development of wide-gap cells poses the largest hurdle, as their efficiencies, despite some progress over the past years, are still unsatisfactory, especially in comparison with perovskite cells of similar bandgap (Figure 6c). Consequently, the efficiency of all-organic tandem solar cells has only slowly improved over the last years and reached values slightly above 20%.[170-173] Additionally, the necessity to absorb high energy photons might lead to stability concerns in organic cells, as discussed above. On the other hand, all-perovskite tandem solar cells have already demonstrated impressive efficiencies beyond 29%.[1,174] Narrow-bandgap perovskite absorbers, however, still rely on the partial replacement of lead by tin.[175-177] The required Sn^{2+} state is unfortunately prone to oxidation and the resulting Sn^{4+} oxidation state causes detrimental self-doping and ultimately compromises device stability.[178,179] Although several strategies have been proposed to mitigate this oxidation,[180-182] the stability of tin-containing perovskite has not shown significant improvement over the past years, in stark contrast to perovskite solar cells exclusively based on lead, which have seen a steady increase of operational lifetime (see Figure 6d).

Since it is still uncertain, if tin oxidation will ultimately turn out as a fundamental roadblock, perovskite-organic tandem solar cells emerge as highly promising candidates, where the strengths of both technologies are combined. The previously discussed challenge to develop efficient and stable wide-bandgap perovskite cells is common to all successful perovskite tandem technologies and will naturally be a focus of research for the entire perovskite tandem community. Surely, the narrow-gap organic solar cell presents a stable alternative for the currently unstable tin-containing perovskite absorbers. As shown in Figure 6e, the vigorous research on novel non-fullerene acceptors has already unleashed an accelerating development of perovskite-organic tandem solar cell efficiencies. Continued progress towards efficient

organic subcells with further lowered energy gap, as illustrated in Figure 6f, will provide an avenue to flexible, lightweight, and low-cost perovskite-organic tandems with an efficiency of 30% and beyond.[28]

References:

1 Green, M. A. *et al.* Solar cell efficiency tables (version 62). *Progress in Photovoltaics: Research and Applications* **31**, 651-663 (2023). https://doi.org:10.1002/pip.3726

2 NREL. *Best Research-Cell Efficiency Chart (accessed 07/23)*.

3 Vos, A. D. Detailed balance limit of the efficiency of tandem solar cells. *Journal of Physics D: Applied Physics* **13**, 839-846 (1980). https://doi.org:10.1088/0022-3727/13/5/018

4 Brinkmann, K. O. *et al.* Perovskite–organic tandem solar cells with indium oxide interconnect. *Nature* **604**, 280-286 (2022). https://doi.org:10.1038/s41586-022-04455-0

5 Wang, X. *et al.* Highly Efficient Perovskite/Organic Tandem Solar Cells Enabled by Mixed-Cation Surface Modulation. *Adv Mater*, e2305946 (2023). https://doi.org:10.1002/adma.202305946

6 Chen, W. *et al.* Monolithic perovskite/organic tandem solar cells with 23.6% efficiency enabled by reduced voltage losses and optimized interconnecting layer. *Nature Energy* **7**, 229-237 (2022). https://doi.org:10.1038/s41560-021-00966-8

7 Yu, G., Gao, J., Hummelen, J. C., Wudl, F. & Heeger, A. J. Polymer Photovoltaic Cells: Enhanced Efficiencies via a Network of Internal Donor-Acceptor Heterojunctions. *Science* **270**, 1789-1791 (1995). https://doi.org:10.1126/science.270.5243.1789

8 Lin, Y. *et al.* An Electron Acceptor Challenging Fullerenes for Efficient Polymer Solar Cells. *Advanced Materials* **27**, 1170-1174 (2015). https://doi.org:10.1002/adma.201404317

9 Zhang, G. *et al.* Delocalization of exciton and electron wavefunction in non-fullerene acceptor molecules enables efficient organic solar cells. *Nature Communications* **11**, 3943 (2020). https://doi.org:10.1038/s41467-020-17867-1

10 Firdaus, Y. *et al.* Long-range exciton diffusion in molecular non-fullerene acceptors. *Nature Communications* **11**, 5220 (2020). https://doi.org:10.1038/s41467-020-19029-9

11 Tokmoldin, N. *et al.* Extraordinarily long diffusion length in PM6:Y6 organic solar cells. *Journal of Materials Chemistry A* **8**, 7854-7860 (2020). https://doi.org:10.1039/d0ta03016c

12 Yuan, J. *et al.* Single-Junction Organic Solar Cell with over 15% Efficiency Using Fused-Ring Acceptor with Electron-Deficient Core. *Joule* **3**, 1140-1151 (2019). https://doi.org:10.1016/j.joule.2019.01.004

13 Zhu, L. *et al.* Single-junction organic solar cells with over 19% efficiency enabled by a refined double-fibril network morphology. *Nature Materials* **21**, 656-663 (2022). https://doi.org:10.1038/s41563-022-01244-y

14 Wang, J. *et al.* Binary Organic Solar Cells with 19.2% Efficiency Enabled by Solid Additive. *Advanced Materials* (2023). https://doi.org:10.1002/adma.202301583

15 Wu, S., Liu, M. & Jen, A. K. Y. Prospects and challenges for perovskite-organic tandem solar cells. *Joule* **7**, 484-502 (2023). https://doi.org:10.1016/j.joule.2023.02.014

16 Zhang, G. *et al.* Renewed Prospects for Organic Photovoltaics. *Chem Rev* **122**, 14180-14274 (2022). https://doi.org:10.1021/acs.chemrev.1c00955

17 Meng, D. *et al.* Near‐Infrared Materials: The Turning Point of Organic Photovoltaics. *Advanced Materials* **34**, 2107330 (2022). https://doi.org:10.1002/adma.202107330

18 Yan, C. *et al.* Non-fullerene acceptors for organic solar cells. *Nature Reviews Materials* **3**, 18003 (2018).

19 Wang, J. & Zhan, X. Fused-Ring Electron Acceptors for Photovoltaics and Beyond. *Accounts of Chemical Research* **54**, 132-143 (2021). https://doi.org:10.1021/acs.accounts.0c00575

20 Wang, J., Xue, P., Jiang, Y., Huo, Y. & Zhan, X. The principles, design and applications of fused-ring electron acceptors. *Nature Reviews Chemistry* **6**, 614-634 (2022). https://doi.org:10.1038/s41570-022-00409-2

21 Cheng, P. & Yang, Y. Narrowing the Band Gap: The Key to High-Performance Organic Photovoltaics. *Accounts of Chemical Research* **53**, 1218-1228 (2020). https://doi.org:10.1021/acs.accounts.0c00157

22 Hou, J., Inganäs, O., Friend, R. H. & Gao, F. Organic solar cells based on non-fullerene acceptors. *Nature Materials* **17**, 119-128 (2018). https://doi.org:10.1038/nmat5063

23 Li, C. *et al.* Non-fullerene acceptors with branched side chains and improved molecular packing to exceed 18% efficiency in organic solar cells. *Nature Energy* **6**, 605-613 (2021). https://doi.org:10.1038/s41560-021-00820-x

24 Zhu, Y. *et al.* Rational Strategy to Stabilize an Unstable High‐Efficiency Binary Nonfullerene Organic Solar Cells with a Third Component. *Advanced Energy Materials* **9**, 1900376 (2019). https://doi.org:10.1002/aenm.201900376

25 Qin, Y. *et al.* The performance-stability conundrum of BTP-based organic solar cells. *Joule* **5**, 2129-2147 (2021). https://doi.org:10.1016/j.joule.2021.06.006

26 Weitz, P. *et al.* Revealing Photodegradation Pathways of Organic Solar Cells by Spectrally Resolved Accelerated Lifetime Analysis. *Advanced Energy Materials* **13**, 2202564 (2023). https://doi.org:10.1002/aenm.202202564

27 Liu, T. *et al.* Photochemical Decomposition of Y‐Series Non‐Fullerene Acceptors Is Responsible for Degradation of High‐Efficiency Organic Solar Cells. *Advanced Energy Materials* **13**, 2300046 (2023). https://doi.org:10.1002/aenm.202300046

28 Jia, Z. *et al.* Near-infrared absorbing acceptor with suppressed triplet exciton generation enabling high performance tandem organic solar cells. *Nature Communications* **14** (2023). https://doi.org:10.1038/s41467-023-36917-y

29 Ho-Baillie, A. W. Y. *et al.* Recent progress and future prospects of perovskite tandem solar cells. *Applied Physics Reviews* **8**, 041307 (2021). https://doi.org:10.1063/5.0061483

30 Caspar, J. V. & Meyer, T. J. Application of the energy gap law to nonradiative, excited-state decay. *The Journal of Physical Chemistry* **87**, 952-957 (1983). https://doi.org:10.1021/j100229a010

31 Englman, R. & Jortner, J. The energy gap law for radiationless transitions in large molecules. *Molecular Physics* **18**, 145-164 (1970). https://doi.org:10.1080/00268977000100171

32 Tokmoldin, N. *et al.* Explaining the Fill‐Factor and Photocurrent Losses of Nonfullerene Acceptor‐Based Solar Cells by Probing the Long‐Range Charge Carrier Diffusion and Drift Lengths. *Advanced Energy Materials* **11**, 2100804 (2021). https://doi.org:10.1002/aenm.202100804

33 Schopp, N. *et al.* Understanding Interfacial Recombination Processes in Narrow-Band-Gap Organic Solar Cells. *ACS Energy Letters* **7**, 1626-1634 (2022). https://doi.org:10.1021/acsenergylett.2c00502

34 Zhou, B. *et al.* On the Stability of Non‐fullerene Acceptors and Their Corresponding Organic Solar Cells: Influence of Side Chains. *Advanced Functional Materials* **32**, 2206042 (2022). https://doi.org:10.1002/adfm.202206042

35 Hu, H. *et al.* The Role of Demixing and Crystallization Kinetics on the Stability of Non‐Fullerene Organic Solar Cells. *Advanced Materials* **32**, 2005348 (2020). https://doi.org:10.1002/adma.202005348

36 Zhou, K., Xin, J. & Ma, W. Hierarchical Morphology Stability under Multiple Stresses in Organic Solar Cells. *ACS Energy Letters* **4**, 447-455 (2019). https://doi.org:10.1021/acsenergylett.8b02383

37 Zhang, K.-N. *et al.* High‐Performance Ternary Organic Solar Cells with Morphology‐Modulated Hole Transfer and Improved Ultraviolet Photostability. *Solar RRL* **4**, 2000165 (2020). https://doi.org:10.1002/solr.202000165

38 Peng, Z., Stingelin, N., Ade, H. & Michels, J. J. A materials physics perspective on structure–processing–function relations in blends of organic semiconductors. *Nature Reviews Materials* **8**, 439–455 (2023). https://doi.org:10.1038/s41578-023-00541-5

39 Ye, L. *et al.* Quantitative relations between interaction parameter, miscibility and function in organic solar cells. *Nature Materials* **17**, 253-260 (2018). https://doi.org:10.1038/s41563-017-0005-1

40 Peng, Z. & Ade, H. Unveiling re-entrant phase behavior and crystalline–amorphous interactions in semi-conducting polymer:small molecule blends. *Materials Horizons*, 2698-2705 (2023). https://doi.org:10.1039/d3mh00034f

41 Ghasemi, M. *et al.* A molecular interaction–diffusion framework for predicting organic solar cell stability. *Nature Materials* **20**, 525-532 (2021). https://doi.org:10.1038/s41563-020-00872-6

42 Ye, L. *et al.* Quenching to the Percolation Threshold in Organic Solar Cells. *Joule* **3**, 443-458 (2019). https://doi.org:10.1016/j.joule.2018.11.006

43 Wienhold, K. S. *et al.* Effect of Solvent Additives on the Morphology and Device Performance of Printed Nonfullerene Acceptor Based Organic Solar Cells. *ACS Applied Materials & Interfaces* **11**, 42313-42321 (2019). https://doi.org:10.1021/acsami.9b16784

44 He, Q. *et al.* Revealing Morphology Evolution in Highly Efficient Bulk Heterojunction and Pseudo‐Planar Heterojunction Solar Cells by Additives Treatment. *Advanced Energy Materials* **11**, 2003390 (2021). https://doi.org:10.1002/aenm.202003390

45 Wang, X. *et al.* High‐Efficiency (16.93%) Pseudo‐Planar Heterojunction Organic Solar Cells Enabled by Binary Additives Strategy. *Advanced Functional Materials* **31**, 2102291 (2021). https://doi.org:10.1002/adfm.202102291

46 Gasparini, N., Salleo, A., McCulloch, I. & Baran, D. The role of the third component in ternary organic solar cells. *Nature Reviews Materials* **4**, 229-242 (2019). https://doi.org:10.1038/s41578-019-0093-4

47 Pan, M.-A. *et al.* 16.7%-efficiency ternary blended organic photovoltaic cells with PCBM as the acceptor additive to increase the open-circuit voltage and phase purity. *Journal of Materials Chemistry A* **7**, 20713-20722 (2019). https://doi.org:10.1039/C9TA06929A

48 Liu, F. *et al.* Ternary organic solar cells based on polymer donor, polymer acceptor and PCBM components. *Chinese Chemical Letters* **31**, 865-868 (2020). https://doi.org:https://doi.org/10.1016/j.cclet.2019.06.051

49 Hoppe, H. & Sariciftci, N. S. Organic solar cells: An overview. *Journal of Materials Research* **19**, 1924-1945 (2004). https://doi.org:10.1557/jmr.2004.0252

50 Neugebauer, H., Brabec, C., Hummelen, J. C. & Sariciftci, N. S. Stability and photodegradation mechanisms of conjugated polymer/fullerene plastic solar cells. *Solar Energy Materials and Solar Cells* **61**, 35-42 (2000). https://doi.org:10.1016/s0927-0248(99)00094-x

51 Günes, S., Neugebauer, H. & Sariciftci, N. S. Conjugated Polymer-Based Organic Solar Cells. *Chemical Reviews* **107**, 1324-1338 (2007). https://doi.org:10.1021/cr050149z

52 Tang, H. *et al.* Interface Engineering for Highly Efficient Organic Solar Cells. *Advanced Materials*, 2212236 (2023). https://doi.org:10.1002/adma.202212236

53 Jiang, Y. *et al.* Photocatalytic effect of ZnO on the stability of nonfullerene acceptors and its mitigation by SnO₂for nonfullerene organic solar cells. *Materials Horizons* **6**, 1438-1443 (2019). https://doi.org:10.1039/c9mh00379g

54 Jiang, P. *et al.* On the interface reactions and stability of nonfullerene organic solar cells. *Chemical Science* **13**, 4714-4739 (2022). https://doi.org:10.1039/d1sc07269b

55 Zilberberg, K., Gharbi, H., Behrendt, A., Trost, S. & Riedl, T. Low-Temperature, Solution-Processed MoO_x for Efficient and Stable Organic Solar Cells. *ACS Applied Materials & Interfaces* **4**, 1164-1168 (2012). https://doi.org:10.1021/am201825t

56 Jørgensen, M., Norrman, K. & Krebs, F. C. Stability/degradation of polymer solar cells. *Solar Energy Materials and Solar Cells* **92**, 686-714 (2008). https://doi.org:10.1016/j.solmat.2008.01.005

57 Jørgensen, M. *et al.* Stability of Polymer Solar Cells. *Advanced Materials* **24**, 580-612 (2012). https://doi.org:10.1002/adma.201104187

58 Wang, Y. *et al.* The critical role of the donor polymer in the stability of high-performance non-fullerene acceptor organic solar cells. *Joule* **7**, 810-829 (2023). https://doi.org:https://doi.org/10.1016/j.joule.2023.03.002

59 Zhou, Y., Poli, I., Meggiolaro, D., De Angelis, F. & Petrozza, A. Defect activity in metal halide perovskites with wide and narrow bandgap. *Nature Reviews Materials* **6**, 986-1002 (2021). https://doi.org:10.1038/s41578-021-00331-x

60 He, R. *et al.* Wide-bandgap organic–inorganic hybrid and all-inorganic perovskite solar cells and their application in all-perovskite tandem solar cells. *Energy & Environmental Science* **14**, 5723-5759 (2021). https://doi.org:10.1039/d1ee01562a

61 Nie, T., Fang, Z., Ren, X., Duan, Y. & Liu, S. Recent Advances in Wide-Bandgap Organic–Inorganic Halide Perovskite Solar Cells and Tandem Application. *Nano-Micro Letters* **15** (2023). https://doi.org:10.1007/s40820-023-01040-6

62 Motti, S. G. *et al.* Phase segregation in mixed-halide perovskites affects charge-carrier dynamics while preserving mobility. *Nature Communications* **12**, 6955 (2021). https://doi.org:10.1038/s41467-021-26930-4

63 Hoke, E. T. *et al.* Reversible photo-induced trap formation in mixed-halide hybrid perovskites for photovoltaics. *Chemical Science* **6**, 613-617 (2015). https://doi.org:10.1039/c4sc03141e

64 Knight, A. J. & Herz, L. M. Preventing phase segregation in mixed-halide perovskites: a perspective. *Energy and Environmental Science* **13**, 2024-2046 (2020). https://doi.org:10.1039/d0ee00788a

65 Tong, Y. *et al.* Wide‐Bandgap Organic–Inorganic Lead Halide Perovskite Solar Cells. *Advanced Science* **9**, 2105085 (2022). https://doi.org:10.1002/advs.202105085

66 Mahesh, S. *et al.* Revealing the origin of voltage loss in mixed-halide perovskite solar cells. *Energy & Environmental Science* **13**, 258-267 (2020). https://doi.org:10.1039/c9ee02162k

67 Caprioglio, P. *et al.* Nano-emitting Heterostructures Violate Optical Reciprocity and Enable Efficient Photoluminescence in Halide-Segregated Methylammonium-Free Wide Bandgap Perovskites. *ACS Energy Letters* **6**, 419-428 (2021). https://doi.org:10.1021/acsenergylett.0c02270

68 Thiesbrummel, J. *et al.* Ion induced field screening governs the early performance degradation of perovskite solar cells. *Research Square Platform LLC* (2023). https://doi.org:10.21203/rs.3.rs-2495973/v1

69 Peña-Camargo, F. *et al.* Halide Segregation versus Interfacial Recombination in Bromide-Rich Wide-Gap Perovskite Solar Cells. *ACS Energy Letters* **5**, 2728-2736 (2020). https://doi.org:10.1021/acsenergylett.0c01104

70 Yao, Q. *et al.* Dual Sub‐Cells Modification Enables High‐Efficiency n‐i‐p Type Monolithic Perovskite/Organic Tandem Solar Cells. *Advanced Functional Materials* **33**, 2212599 (2023). https://doi.org:10.1002/adfm.202212599

71 Lai, H. *et al.* High‐Performance Flexible All‐Perovskite Tandem Solar Cells with Reduced V_{OC}-Deficit in Wide‐Bandgap Subcell. *Advanced Energy Materials* **12**, 2202438 (2022). https://doi.org:10.1002/aenm.202202438

72 Chen, H. *et al.* Regulating surface potential maximizes voltage in all-perovskite tandems. *Nature* **613**, 676-681 (2023). https://doi.org:10.1038/s41586-022-05541-z

73 Wang, C. *et al.* Suppressing Phase Segregation in Wide Bandgap Perovskites for Monolithic Perovskite/Organic Tandem Solar Cells with Reduced Voltage Loss. *Small* **18**, 2204081 (2022). https://doi.org:10.1002/smll.202204081

74 Thiesbrummel, J. *et al.* Understanding and Minimizing V_{OC} Losses in All‐Perovskite Tandem Photovoltaics. *Advanced Energy Materials* **13**, 2202674 (2023). https://doi.org:10.1002/aenm.202202674

75 Brennan, M. C., Draguta, S., Kamat, P. V. & Kuno, M. Light-Induced Anion Phase Segregation in Mixed Halide Perovskites. *ACS Energy Letters* **3**, 204-213 (2017). https://doi.org:10.1021/acsenergylett.7b01151

76 Datta, K. *et al.* Light-Induced Halide Segregation in 2D and Quasi-2D Mixed-Halide Perovskites. *ACS Energy Letters* **8**, 1662-1670 (2023). https://doi.org:10.1021/acsenergylett.3c00160

77 Kamat, P. V. & Kuno, M. Halide Ion Migration in Perovskite Nanocrystals and Nanostructures. *Accounts of Chemical Research* **54**, 520-531 (2021). https://doi.org:10.1021/acs.accounts.0c00749

78 Brinkmann, K. O. *et al.* Suppressed decomposition of organometal halide perovskites by impermeable electron-extraction layers in inverted solar cells. *Nature Communications* **8**, 13938 (2017). https://doi.org:10.1038/ncomms13938

79 Kato, Y. *et al.* Silver Iodide Formation in Methyl Ammonium Lead Iodide Perovskite Solar Cells with Silver Top Electrodes. *Advanced Materials Interfaces* **2**, 1500195 (2015). https://doi.org:10.1002/admi.201500195

80 Sakhatskyi, K. *et al.* Assessing the Drawbacks and Benefits of Ion Migration in Lead Halide Perovskites. *ACS Energy Letters* **7**, 3401-3414 (2022). https://doi.org:10.1021/acsenergylett.2c01663

81 Zhao, Y., Zhou, W., Han, Z., Yu, D. & Zhao, Q. Effects of ion migration and improvement strategies for the operational stability of perovskite solar cells. *Physical Chemistry Chemical Physics* **23**, 94-106 (2021). https://doi.org:10.1039/d0cp04418k

82 Kerner, R. A., Xu, Z., Larson, B. W. & Rand, B. P. The role of halide oxidation in perovskite halide phase separation. *Joule* **5**, 2273-2295 (2021). https://doi.org:10.1016/j.joule.2021.07.011

83 Wright, A. D., Patel, J. B., Johnston, M. B. & Herz, L. M. Temperature‐Dependent Reversal of Phase Segregation in Mixed‐Halide Perovskites. *Advanced Materials* **35**, 2210834 (2023). https://doi.org:10.1002/adma.202210834

84 Choe, H., Jeon, D., Lee, S. J. & Cho, J. Mixed or Segregated: Toward Efficient and Stable Mixed Halide Perovskite-Based Devices. *ACS Omega* **6**, 24304-24315 (2021). https://doi.org:10.1021/acsomega.1c03714

85 Zhao, Y. *et al.* Strain-activated light-induced halide segregation in mixed-halide perovskite solids. *Nature Communications* **11**, 6328 (2020). https://doi.org:10.1038/s41467-020-20066-7

86 Elmelund, T., Seger, B., Kuno, M. & Kamat, P. V. How Interplay between Photo and Thermal Activation Dictates Halide Ion Segregation in Mixed Halide Perovskites. *ACS Energy Letters* **5**, 56-63 (2020). https://doi.org:10.1021/acsenergylett.9b02265

87 Belisle, R. A. *et al.* Impact of Surfaces on Photoinduced Halide Segregation in Mixed-Halide Perovskites. *ACS Energy Letters* **3**, 2694-2700 (2018).

88 Dubose, J. T. & Kamat, P. V. Hole Trapping in Halide Perovskites Induces Phase Segregation. *Accounts of Materials Research* **3**, 761-771 (2022). https://doi.org:10.1021/accountsmr.2c00076

89 Knight, A. J. *et al.* Electronic Traps and Phase Segregation in Lead Mixed-Halide Perovskite. *ACS Energy Letters* **4**, 75-84 (2019). https://doi.org:10.1021/acsenergylett.8b02002

90 Knight, A. J., Patel, J. B., Snaith, H. J., Johnston, M. B. & Herz, L. M. Trap States, Electric Fields, and Phase Segregation in Mixed‐Halide Perovskite Photovoltaic Devices. *Advanced Energy Materials* **10**, 1903488 (2020). https://doi.org:10.1002/aenm.201903488

91 Wang, S., Wang, A. & Hao, F. Toward stable lead halide perovskite solar cells: A knob on the A/X sites components. *iScience* **25**, 103599 (2022). https://doi.org:10.1016/j.isci.2021.103599

92 Xu, Z., Kerner, R. A., Berry, J. J. & Rand, B. P. Iodine Electrochemistry Dictates Voltage‐Induced Halide Segregation Thresholds in Mixed‐Halide Perovskite Devices. *Advanced Functional Materials* **32**, 2203432 (2022). https://doi.org:10.1002/adfm.202203432

93 Mathew, P. S., Szabó, G., Kuno, M. & Kamat, P. V. Phase Segregation and Sequential Expulsion of Iodide and Bromide in Photoirradiated Ruddlesden–Popper 2D Perovskite Films. *ACS Energy Letters* **7**, 3982-3988 (2022). https://doi.org:10.1021/acsenergylett.2c02026

94 Duong, T. *et al.* Light and Electrically Induced Phase Segregation and Its Impact on the Stability of Quadruple Cation High Bandgap Perovskite Solar Cells. *ACS Appl Mater Interfaces* **9**, 26859-26866 (2017). https://doi.org:10.1021/acsami.7b06816

95 Yin, W.-J., Shi, T. & Yan, Y. Unusual defect physics in $CH_3NH_3PbI_3$ perovskite solar cell absorber. *Applied Physics Letters* **104** (2014). https://doi.org:10.1063/1.4864778

96 Tao, S. *et al.* Absolute energy level positions in tin- and lead-based halide perovskites. *Nature Communications* **10**, 2560 (2019). https://doi.org:10.1038/s41467-019-10468-7

97 Kim, D. *et al.* Microstructural Evaluation of Phase Instability in Large Bandgap Metal Halide Perovskites. *ACS Nano* **15**, 20391-20402 (2021). https://doi.org:10.1021/acsnano.1c08726

98 Knight, A. J. *et al.* Halide Segregation in Mixed-Halide Perovskites: Influence of A-Site Cations. *ACS Energy Letters* **6**, 799-808 (2021). https://doi.org:10.1021/acsenergylett.0c02475

99 Wang, Z. *et al.* Recent Advances and Perspectives of Photostability for Halide Perovskite Solar Cells. *Advanced Optical Materials* **10**, 2101822 (2022). https://doi.org:10.1002/adom.202101822

100 Zheng, Y. *et al.* Downward Homogenized Crystallization for Inverted Wide‐Bandgap Mixed‐Halide Perovskite Solar Cells with 21% Efficiency and Suppressed Photo‐Induced Halide Segregation. *Advanced Functional Materials* **32**, 2200431 (2022). https://doi.org:10.1002/adfm.202200431

101 Tao, L. *et al.* Stability of mixed-halide wide bandgap perovskite solar cells: Strategies and progress. *Journal of Energy Chemistry* **61**, 395-415 (2021). https://doi.org:10.1016/j.jechem.2021.03.038

102 Rehman, W. *et al.* Photovoltaic mixed-cation lead mixed-halide perovskites: links between crystallinity, photo-stability and electronic properties. *Energy and Environmental Science* **10**, 361-369 (2017). https://doi.org:10.1039/c6ee03014a

103 Jiang, Q. *et al.* Compositional texture engineering for highly stable wide-bandgap perovskite solar cells. *Science* **378**, 1295-1300 (2022). https://doi.org:doi:10.1126/science.adf0194

104 Levine, I. *et al.* Charge transfer rates and electron trapping at buried interfaces of perovskite solar cells. *Joule* **5**, 2915-2933 (2021). https://doi.org:10.1016/j.joule.2021.07.016

105 Lim, V. J. Y. *et al.* Impact of Hole‐Transport Layer and Interface Passivation on Halide Segregation in Mixed‐Halide Perovskites. *Advanced Functional Materials* **32**, 2204825 (2022). https://doi.org:10.1002/adfm.202204825

106 Al-Ashouri, A. *et al.* Monolithic perovskite/silicon tandem solar cell with 29% efficiency by enhanced hole extraction. *Science* **370**, 1300-1309 (2020).

107 Xia, J., Sohail, M. & Nazeeruddin, M. K. Efficient and Stable Perovskite Solar Cells by Tailoring of Interfaces. *Advanced Materials* **35**, 2211324 (2023). https://doi.org:10.1002/adma.202211324

108 Luo, P. *et al.* Colorful, bandgap-tunable, and air-stable $CsPb(I_xBr_{1-x})_3$ inorganic perovskite films via a novel sequential chemical vapor deposition. *Ceramics International* **44**, 12783-12788 (2018). https://doi.org:https://doi.org/10.1016/j.ceramint.2018.04.084

109 Kulkarni, S. A. *et al.* Band-gap tuning of lead halide perovskites using a sequential deposition process. *J. Mater. Chem. A* **2**, 9221-9225 (2014). https://doi.org:10.1039/c4ta00435c

110 Bush, K. A. *et al.* Compositional Engineering for Efficient Wide Band Gap Perovskites with Improved Stability to Photoinduced Phase Segregation. *ACS Energy Letters* **3**, 428-435 (2018). https://doi.org:10.1021/acsenergylett.7b01255

111 Xiang, W., Liu, S. & Tress, W. A review on the stability of inorganic metal halide perovskites: challenges and opportunities for stable solar cells. *Energy & Environmental Science* **14**, 2090-2113 (2021). https://doi.org:10.1039/D1EE00157D

112 Zhao, X. *et al.* Accelerated aging of all-inorganic, interface-stabilized perovskite solar cells. *Science* **377**, 307-310 (2022). https://doi.org:10.1126/science.abn5679

113 Li, T. *et al.* Inorganic wide-bandgap perovskite subcells with dipole bridge for all-perovskite tandems. *Nature Energy* **8**, 610-620 (2023). https://doi.org:10.1038/s41560-023-01250-7

114 Wang, P. *et al.* Tuning of the Interconnecting Layer for Monolithic Perovskite/Organic Tandem Solar Cells with Record Efficiency Exceeding 21%. *Nano Letters* **21**, 7845-7854 (2021). https://doi.org:10.1021/acs.nanolett.1c02897

115 Mariotti, S. *et al.* Stability and Performance of CsPbI2Br Thin Films and Solar Cell Devices. *ACS Applied Materials & Interfaces* **10**, 3750-3760 (2018). https://doi.org:10.1021/acsami.7b14039

116 Ji, S. G. *et al.* Stable pure-iodide wide-band-gap perovskites for efficient Si tandem cells via kinetically controlled phase evolution. *Joule* **6**, 2390-2405 (2022). https://doi.org:10.1016/j.joule.2022.08.006

117 Cariou, R. *et al.* III–V-on-silicon solar cells reaching 33% photoconversion efficiency in two-terminal configuration. *Nature Energy* **3**, 326-333 (2018). https://doi.org:10.1038/s41560-018-0125-0

118 Kröger, M. *et al.* Role of the deep-lying electronic states of MoO_3 in the enhancement of hole-injection in organic thin films. *Applied Physics Letters* **95**, 123301 (2009). https://doi.org:10.1063/1.3231928

119 Meyer, J. *et al.* Transition Metal Oxides for Organic Electronics: Energetics, Device Physics and Applications. *Advanced Materials* **24**, 5408-5427 (2012). https://doi.org:10.1002/adma.201201630

120 Becker, T. *et al.* All-Oxide MoO_x / SnO_x Charge Recombination Interconnects for Inverted Organic Tandem Solar Cells. *Advanced Energy Materials* **8**, 1702533 (2018). https://doi.org:10.1002/aenm.201702533

121 Gahlmann, T. *et al.* Impermeable Charge Transport Layers Enable Aqueous Processing on Top of Perovskite Solar Cells. *Advanced Energy Materials* **10**, 1903897 (2020). https://doi.org:10.1002/aenm.201903897

122 Hoffmann, L. *et al.* Spatial Atmospheric Pressure Atomic Layer Deposition of Tin Oxide as an Impermeable Electron Extraction Layer for Perovskite Solar Cells with Enhanced Thermal Stability. *ACS Applied Materials and Interfaces* **10**, 6006–6013 (2018). https://doi.org:10.1021/acsami.7b17701

123 Wang, Y.-L. *et al.* Room temperature deposited indium zinc oxide thin film transistors. *Applied Physics Letters* **90**, 232103 (2007). https://doi.org:10.1063/1.2746084

124 Lany, S. *et al.* Surface Origin of High Conductivities in Undoped In_2O_3 Thin Films. *Physical Review Letters* **108**, 016802 (2012). https://doi.org:10.1103/PhysRevLett.108.016802

125 Kibis, L. S. *et al.* The investigation of oxidized silver nanoparticles prepared by thermal evaporation and radio-frequency sputtering of metallic silver under oxygen. *Applied Surface Science* **257**, 404-413 (2010). https://doi.org:https://doi.org/10.1016/j.apsusc.2010.07.002

126 Raffi, M., Rumaiz, A. K., Hasan, M. M. & Shah, S. I. Studies of the growth parameters for silver nanoparticle synthesis by inert gas condensation. *Journal of Materials Research* **22**, 3378-3384 (2007). https://doi.org:10.1557/jmr.2007.0420

127 Trost, S. *et al.* Plasmonically sensitized metal-oxide electron extraction layers for organic solar cells. *Scientific Reports* **5**, 7765 (2015). https://doi.org:10.1038/srep07765

128 Polywka, A., Vereshchaeva, A., Riedl, T. & Görrn, P. Manipulating the Morphology of Silver Nanoparticles with Local Plasmon-Mediated Control. *Particle & Particle Systems Characterization* **31**, 342-346 (2014). https://doi.org:10.1002/ppsc.201300175

129 Martínez-Otero, A., Liu, Q., Mantilla-Perez, P., Bajo, M. M. & Martorell, J. An extremely thin and robust interconnecting layer providing 76% fill factor in a tandem polymer solar cell architecture. *Journal of Materials Chemistry A* **3**, 10681-10686 (2015). https://doi.org:10.1039/c5ta02205c

130 Yang, H. *et al.* Regulating Charge Carrier Recombination in the Interconnecting Layer to Boost the Efficiency and Stability of Monolithic Perovskite/Organic Tandem Solar Cells. *Advanced Materials* **35**, 2208604 (2023). https://doi.org:10.1002/adma.202208604

131 Sun, S. Q. *et al.* All‐Inorganic Perovskite‐Based Monolithic Perovskite/Organic Tandem Solar Cells with 23.21% Efficiency by Dual‐Interface Engineering. *Advanced Energy Materials*, 2204347 (2023). https://doi.org:10.1002/aenm.202204347

132 Schloemer, T. H. *et al.* The Molybdenum Oxide Interface Limits the High-Temperature Operational Stability of Unencapsulated Perovskite Solar Cells. *ACS Energy Letters* **5**, 2349-2360 (2020). https://doi.org:10.1021/acsenergylett.0c01023

133 Meyer, J., Zilberberg, K., Riedl, T. & Kahn, A. Electronic structure of Vanadium pentoxide: An efficient hole injector for organic electronic materials. *Journal of Applied Physics* **110** (2011). https://doi.org:10.1063/1.3611392

134 Abdollahi Nejand, B. *et al.* Scalable two-terminal all-perovskite tandem solar modules with a 19.1% efficiency. *Nature Energy* **7**, 620-630 (2022). https://doi.org:10.1038/s41560-022-01059-w

135 Yu, Z. *et al.* Simplified interconnection structure based on C60/SnO2-x for all-perovskite tandem solar cells. *Nature Energy* **5**, 657-665 (2020). https://doi.org:10.1038/s41560-020-0657-y

136 Brinkmann, K. O., Gahlmann, T. & Riedl, T. Atomic Layer Deposition of Functional Layers in Planar Perovskite Solar Cells. *Solar RRL* **4**, 1900332 (2020). https://doi.org:10.1002/solr.201900332

137 Behrendt, A. *et al.* Highly robust transparent and conductive gas diffusion barriers based on tin oxide. *Adv Mater* **27**, 5961-5967 (2015). https://doi.org:10.1002/adma.201502973

138 Zhao, J. *et al.* Self-Encapsulating Thermostable and Air-Resilient Semitransparent Perovskite Solar Cells. *Advanced Energy Materials* **7**, 1602599 (2017). https://doi.org:10.1002/aenm.201602599

139 Ruben, G. C. Ultrathin (1 nm) vertically shadowed platinum-carbon replicas for imaging individual molecules in freeze-etched biological DNA and material science metal and plastic specimens. *Journal of Electron Microscopy Technique* **13**, 335-354 (1989). https://doi.org:10.1002/jemt.1060130407

140 Hoffmann, L. *et al.* Atmospheric pressure plasma enhanced spatial atomic layer deposition of SnO_x as conductive gas diffusion barrier. *Journal of Vacuum Science & Technology A* **36**, 01A112 (2018). https://doi.org:10.1116/1.5006781

141 Illiberi, A. *et al.* Atmospheric plasma-enhanced spatial-ALD of InZnO for high mobility thin film transistors. *Journal of Vacuum Science & Technology A* **36**, 04F401 (2018). https://doi.org:10.1116/1.5008464

142 Katsouras, I., Frijters, C., Poodt, P., Gelinck, G. & Kronemeijer, A. J. Large‐area spatial atomic layer deposition of amorphous oxide semiconductors at atmospheric pressure. *Journal of the Society for Information Display* **27**, 304-312 (2019). https://doi.org:10.1002/jsid.783

143 Zhao, M.-J. *et al.* Properties and Mechanism of PEALD-In_2O_3 Thin Films Prepared by Different Precursor Reaction Energy. *Nanomaterials* **11**, 978 (2021). https://doi.org:10.3390/nano11040978

144 Kim, D.-H. *et al.* Separation of extremely small indium oxide quantum dots and their highly luminescent properties by dispersing agent. *Journal of Alloys and Compounds* **921**, 166073 (2022). https://doi.org:https://doi.org/10.1016/j.jallcom.2022.166073

145 Granada-Ramirez, D. A. *et al.* Chemical synthesis and optical, structural, and surface characterization of InP-In2O3 quantum dots. *Applied Surface Science* **530**, 147294 (2020). https://doi.org:https://doi.org/10.1016/j.apsusc.2020.147294

146 Wang, J. *et al.* Optical generation of high carrier densities in 2D semiconductor heterobilayers. *Science Advances* **5**, eaax0145 https://doi.org:10.1126/sciadv.aax0145

147 Zhou, X. *et al.* Integrated Ideal‐Bandgap Perovskite/Bulk‐Heterojunction Solar Cells with Efficiencies > 24%. *Advanced Materials* **34**, 2205809 (2022). https://doi.org:10.1002/adma.202205809

148 Zhang, M. *et al.* Integrated Perovskite/Organic Photovoltaics with Ultrahigh Photocurrent and Photoresponse Approaching 1000 nm. *Solar RRL* **4**, 2000140 (2020). https://doi.org:10.1002/solr.202000140

149 Wang, P., Zhao, Y. & Wang, T. Recent progress and prospects of integrated perovskite/organic solar cells. *Applied Physics Reviews* **7**, 031303 (2020). https://doi.org:10.1063/5.0013912

150 Liu, Y. *et al.* Integrated Perovskite/Bulk-Heterojunction toward Efficient Solar Cells. *Nano Letters* **15**, 662-668 (2015). https://doi.org:10.1021/nl504168q

151 Daboczi, M. *et al.* Towards Efficient Integrated Perovskite/Organic Bulk Heterojunction Solar Cells: Interfacial Energetic Requirement to Reduce Charge Carrier Recombination Losses. *Advanced Functional Materials* **30**, 2001482 (2020). https://doi.org:10.1002/adfm.202001482

152 Hong, S. & Lee, J. Recent Advances and Challenges toward Efficient Perovskite/Organic Integrated Solar Cells. *Energies* **16**, 266 (2022). https://doi.org:10.3390/en16010266

153 Cai, Z. *et al.* Suppressing interface charge recombination for efficient integrated perovskite/organic bulk-heterojunction solar cells. *Journal of Power Sources* **541**, 231665 (2022). https://doi.org:10.1016/j.jpowsour.2022.231665

154 Zuo, C. & Ding, L. Bulk heterojunctions push the photoresponse of perovskite solar cells to 970 nm. *Journal of Materials Chemistry A* **3**, 9063-9066 (2015). https://doi.org:10.1039/c4ta04482g

155 Liu, Y. & Chen, Y. Integrated Perovskite/Bulk‐Heterojunction Organic Solar Cells. *Advanced Materials* **32**, 1805843 (2020). https://doi.org:10.1002/adma.201805843

156 Dong, S. *et al.* Unraveling the High Open Circuit Voltage and High Performance of Integrated Perovskite/Organic Bulk-Heterojunction Solar Cells. *Nano Letters* **17**, 5140-5147 (2017). https://doi.org:10.1021/acs.nanolett.7b02532

157 He, X. *et al.* Enhancing Photoresponse and Photocurrent of Integrated Perovskite/Organic Solar Cells via Layer-by-Layer Processing. *ACS Applied Energy Materials* **6**, 981-988 (2023). https://doi.org:10.1021/acsaem.2c03425

158 Chen, W. *et al.* High Short-Circuit Current Density via Integrating the Perovskite and Ternary Organic Bulk Heterojunction. *ACS Energy Letters* **4**, 2535-2536 (2019). https://doi.org:10.1021/acsenergylett.9b01964

159 Wu, Y. *et al.* Toward Broad Spectral Response Inverted Perovskite Solar Cells: Insulating Quantum‐Cutting Perovskite Nanophosphors and Multifunctional Ternary Organic Bulk‐Heterojunction. *Advanced Energy Materials* **12**, 2200005 (2022). https://doi.org:10.1002/aenm.202200005

160 Shi, Z. *et al.* Light Management through Organic Bulk Heterojunction and Carrier Interfacial Engineering for Perovskite Solar Cells with 23.5% Efficiency. *Advanced Functional Materials* **32**, 2203873 (2022). https://doi.org:10.1002/adfm.202203873

161 Wu, S. *et al.* Low‐Bandgap Organic Bulk‐Heterojunction Enabled Efficient and Flexible Perovskite Solar Cells. *Advanced Materials* **33**, 2105539 (2021). https://doi.org:10.1002/adma.202105539

162 Wang, H. *et al.* Photoconductive Charge Transfer Complexes as Charge Transport Layers for High Performance Inverted Perovskite Solar Cells. *Advanced Functional Materials* **32**, 2201935 (2022). https://doi.org:10.1002/adfm.202201935

163 Tian, X., Stranks, S. D. & You, F. Life cycle energy use and environmental implications of high-performance perovskite tandem solar cells. *Science Advances* **6**, eabb0055 (2020). https://doi.org:10.1126/sciadv.abb0055

164 de Wild-Scholten, M. J. Energy payback time and carbon footprint of commercial photovoltaic systems. *Solar Energy Materials and Solar Cells* **119**, 296-305 (2013). https://doi.org:https://doi.org/10.1016/j.solmat.2013.08.037

165 Hengevoss, D., Baumgartner, C., Nisato, G. & Hugi, C. Life Cycle Assessment and eco-efficiency of prospective, flexible, tandem organic photovoltaic module. *Solar Energy* **137**, 317-327 (2016). https://doi.org:10.1016/j.solener.2016.08.025

166 Wagner, L. *et al.* The Resource Demand of Terawatt-Scale Perovskite Tandem Photovoltaics. (2023).

167 Hu, T. *et al.* Indium-Free Perovskite Solar Cells Enabled by Impermeable Tin-Oxide Electron Extraction Layers. *Advanced Materials* **29**, 1606656 (2017). https://doi.org:10.1002/adma.201606656

168 Zilberberg, K. & Riedl, T. Metal-nanostructures – a modern and powerful platform to create transparent electrodes for thin-film photovoltaics. *Journal of Materials Chemistry A* **4**, 14481-14508 (2016). https://doi.org:10.1039/C6TA05286J

169 Reb, L. K. *et al.* Perovskite and Organic Solar Cells on a Rocket Flight. *Joule* **4**, 1880-1892 (2020). https://doi.org:10.1016/j.joule.2020.07.004

170 Yu, R. *et al.* Improved Charge Transport and Reduced Nonradiative Energy Loss Enable Over 16% Efficiency in Ternary Polymer Solar Cells. *Advanced Materials* **31**, 1902302 (2019). https://doi.org:10.1002/adma.201902302

171 Wang, J. *et al.* A Tandem Organic Photovoltaic Cell with 19.6% Efficiency Enabled by Light Distribution Control. *Advanced Materials* **33**, 2102787 (2021). https://doi.org:10.1002/adma.202102787

172 Zheng, Z. *et al.* Tandem Organic Solar Cell with 20.2% Efficiency. *Joule* **6**, 171-184 (2022). https://doi.org:10.1016/j.joule.2021.12.017

173 Wang, J. *et al.* Tandem organic solar cells with 20.6% efficiency enabled by reduced voltage losses. *National Science Review* (2023). https://doi.org:10.1093/nsr/nwad085

174 Lin, R. *et al.* All-perovskite tandem solar cells with 3D/3D bilayer perovskite heterojunction. *Nature*, (early access) (2023). https://doi.org:10.1038/s41586-023-06278-z

175 Li, C. *et al.* Low-bandgap mixed tin–lead iodide perovskites with reduced methylammonium for simultaneous enhancement of solar cell efficiency and stability. *Nature Energy* **5**, 768-776 (2020). https://doi.org:10.1038/s41560-020-00692-7

176 Gu, S. *et al.* Tin and Mixed Lead–Tin Halide Perovskite Solar Cells: Progress and their Application in Tandem Solar Cells. *Advanced Materials* **32**, 1907392 (2020). https://doi.org:10.1002/adma.201907392

177 Prasanna, R. *et al.* Design of low bandgap tin–lead halide perovskite solar cells to achieve thermal, atmospheric and operational stability. *Nature Energy* **4**, 939-947 (2019). https://doi.org:10.1038/s41560-019-0471-6

178 Hu, S., Smith, J. A., Snaith, H. J. & Wakamiya, A. Prospects for Tin-Containing Halide Perovskite Photovoltaics. *Precision Chemistry* **1**, 69-82 (2023). https://doi.org:10.1021/prechem.3c00018

179 Pascual, J. *et al.* Origin of Sn(ii) oxidation in tin halide perovskites. *Materials Advances* **1**, 1066-1070 (2020). https://doi.org:10.1039/d0ma00245c

180 Joy, S. *et al.* How additives for tin halide perovskites influence the Sn^{4+} concentration. *Journal of Materials Chemistry A* **10**, 13278-13285 (2022). https://doi.org:10.1039/d2ta01429g

181 Wang, S. *et al.* Stabilization of Perovskite Lattice and Suppression of S^{2+}/Sn^{4+} Oxidation via Formamidine Acetate for High Efficiency Tin Perovskite Solar Cells. *Advanced Functional Materials* **33**, 2215041 (2023). https://doi.org:10.1002/adfm.202215041

182 Tong, J. *et al.* Carrier control in Sn–Pb perovskites via 2D cation engineering for all-perovskite tandem solar cells with improved efficiency and stability. *Nature Energy* **7**, 642-651 (2022). https://doi.org:10.1038/s41560-022-01046-1